



RESEARCH ARTICLE

DDR WILEY

Further modifications of 1H-pyrrolo[2,3-b]pyridine derivatives as inhibitors of human neutrophil elastase

Maria P. Giovannoni¹ | Niccolò Cantini¹ | Letizia Crocetti¹ | Gabriella Guerrini¹ | Antonella Iacovone¹ | Igor A. Schepetkin² | Claudia Vergelli¹ | Andrei I. Khlebnikov^{3,4} | Mark T. Quinn²

¹NEUROFARBA, Pharmaceutical and Nutraceutical Section, University of Florence, Sesto Fiorentino, Italy

²Department of Microbiology and Immunology, Montana State University, Bozeman, Montana

³Kizhner Research Center, Tomsk Polytechnic University, Tomsk, Russia

⁴Scientific Research Institute of Biological Medicine, Altai State University, Barnaul, Russia

Correspondence

Letizia Crocetti, Dipartimento di NEUROFARBA, Via Ugo Schiff 6, Sesto Fiorentino 50019, Firenze, Italy.
Email: letizia.crocetti@unifi.it

Funding information

Ministry of Education and Science of the Russian Federation, Grant/Award Number: 4.8192.2017/8.9; Montana University System Research Initiative, Grant/Award Number: 51040-MUSRI2015-03; National Institutes of Health IDeA Program COBRE, Grant/Award Number: GM110732; Tomsk Polytechnic University Competitiveness Enhancement Program; USDA National Institute of Food and Agriculture Hatch, Grant/Award Number: 1009546

Abstract

Human neutrophil elastase (HNE) is a potent protease that plays an important physiological role in many processes and is considered to be a multifunctional enzyme. HNE is also involved in a variety of pathologies affecting the respiratory system. Thus, compounds able to inhibit HNE proteolytic activity could represent effective therapeutics. We present here a new series of pyrrolo[2,3-b]pyridine derivatives of our previously reported potent HNE inhibitors. Our results show that position 2 of the pyrrolo[2,3-b]pyridine scaffold must be unsubstituted, and modifications of this position resulted in loss of HNE inhibitory activity. Conversely, the introduction of certain substituents at position 5 was tolerated, with retention of HNE inhibitory activity (IC_{50} = 15–51 nM) after most substitutions, indicating that bulky and/or lipophilic substituents at position 5 probably interact with the large pocket of the enzyme site and allow Michaelis complex formation. The possibility of Michaelis complex formation between Ser195 and the ligand carbonyl group was assessed by molecular docking, and it was found that highly active HNE inhibitors are characterized by geometries favorable for Michaelis complex formation and by relatively short lengths of the proton transfer channel via the catalytic triad.

KEYWORDS

human neutrophil elastase inhibitors, molecular docking, pyrrolo[2,3-b]pyridine

1 | INTRODUCTION

Polymorphonuclear neutrophils represent a large percentage of the circulating leukocyte population and are the most abundant type of white blood cells in human blood. They are also known as granulocytes due to the numerous granules present in their cytoplasm and are characterized by their nuclear morphology, which is segmented into three to five lobes joined together by a thin membrane. These cells play a fundamental role in immune defense against pathogenic organisms and are the first mediators in the inflammatory response (Korkmaz et al., 2010). Neutrophil granules are classified into primary or azurophil,

secondary or specific, tertiary or gelatinase, and secretory (Pham, 2006). Specifically, the azurophil granules contain myeloperoxidase, some bactericidal proteins, and three serine proteases: proteinase 3, cathepsin G, and human neutrophil elastase (HNE), which is a globular glycoprotein of about 30 kDa belonging to the chymotrypsin family. HNE consists of a single polypeptide chain of 218 amino acids, with two asparagine-linked carbohydrate side chains at Asn95 and Asn144 (Lucas et al., 2011). HNE is stabilized by four disulfide bridges and has 19 arginine residues, resulting in an isoelectric point of 10–11. As with other neutrophil serine proteases, HNE plays an important physiological role and is considered a multifunctional

enzyme that contributes to killing of pathogens, inflammatory processes, and maintenance of tissue homeostasis (Pham, 2006). HNE proteolytic activity depends on the catalytic triad consisting of Ser195-His57-Asp102 (Fujinaga et al., 1996).

The proteolytic activity of serine proteases, which is essential for the maintenance of important host functions, can also be harmful if not properly regulated, and a number of regulatory mechanisms are present (Von Nussbaum et al., 2016). For example, these proteases are stored as inactive precursors in specialized compartments, such as azurophil granules for serine proteases. Once active, serine protease activity can be regulated by endogenous inhibitors, such as α 1-antitrypsin (also known as α 1-proteinase inhibitor [α 1-PI]), elafin, and secretory leukocyte protease inhibitor, which inhibit protease activity (Von Nussbaum et al., 2015; Zhong et al., 2017). The involvement of HNE and other neutrophil serine proteases in the development of chronic pulmonary inflammatory diseases, such as chronic obstructive pulmonary disease (COPD), acute lung injury, acute respiratory distress syndrome (ARDS), and cystic fibrosis (CF) is widely documented and correlated with an imbalance between HNE and endogenous inhibitor activity (Polverino et al., 2017).

Recently, we identified and characterized a number of potent HNE inhibitors with differing structural scaffolds (Crocetti et al., 2011; Crocetti et al., 2013; Crocetti et al., 2016; Crocetti et al., 2018; Giovannoni et al., 2016; Giovannoni et al., 2018; Schepetkin, Khlebnikov, & Quinn, 2007; Vergelli et al., 2017). In the most recent studies, we identified HNE inhibitors with a pyrrolo[2,3-b]pyridine scaffold (Crocetti et al., 2018) and found that the most potent compounds exhibited IC_{50} values in the low nanomolar range (14–87 nM) (see Figure 1). Based on these studies, we performed further modifications of the pyrrolo[2,3-b]pyridine scaffold. While keeping the best substituents identified for N-1 (m-toluoyl) and position 3 (CN group), we introduced substituents with different features at position 5 to screen for more potent HNE inhibitors. Additionally, we investigated substitutions at position 2 of the scaffold by shifting CN from the 3 to the 2 position or inserting other groups.

2 | MATERIALS AND METHODS

2.1 | Chemistry

All final compounds were synthesized as reported in Figures 2–4, and the structures were confirmed on the basis of analytical and spectral data. To obtain the 2- or 2,3-disubstituted pyrrolo[2,3-b]pyridines (**2a–e**), we followed the procedures shown in Figure 2. Starting from the previously synthesized compounds **1a–e** (Bahekar et al., 2007; Baltus et al., 2016; Pires et al., 2016; Sandham et al., 2009), we performed benzylation with m-toluoyl chloride and triethylamine in anhydrous dichloromethane, resulting in final compounds **2a–e**. The synthesis of compounds with different substitutions at position 5 is shown in Figures 3 and 4. Figure 3 shows the synthesis of pyrrolo[2,3-b]pyridines substituted with a bromine, chlorine, or nitro group at position 5. The formyl group of intermediates **4a–c** (Ermoli et al., 2009; Nirogi et al., 2012; Xi & Li, 2014), obtained starting from the corresponding

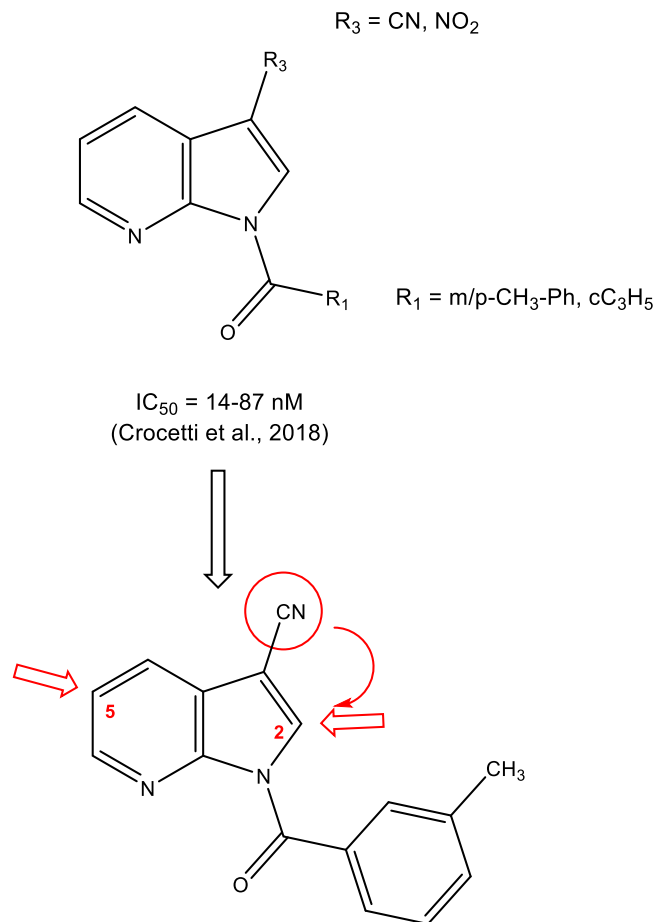


FIGURE 1 Further modifications of the pyrrolo[2,3-b]pyridine scaffold

5-substituted-pyrrolo[2,3-b]pyridines **3a–c** (Bhat et al., 2015; Chen et al., 2015; Joydev et al., 2017) by the Duff reaction, was transformed into the corresponding oxime by treatment with hydroxylamine hydrochloride and $NaHCO_3$ at high temperature, resulting in compounds **5a–c** (5b, Bahekar et al., 2007). Further reaction with $POCl_3$ resulted in the

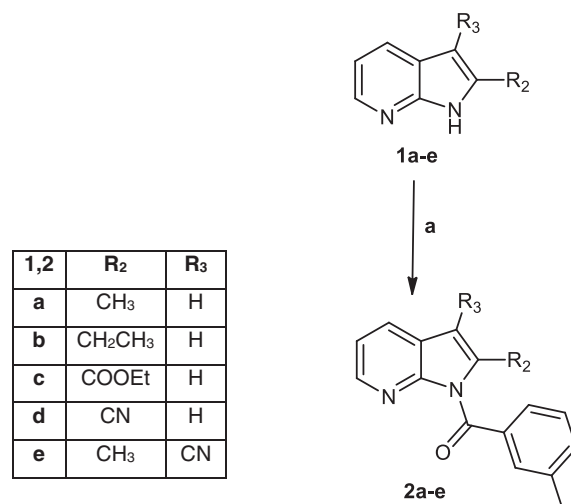


FIGURE 2 Reagents and conditions: (a) *m*-Toluoyl chloride, Et_3N , dry DCM, 0 °C, 2 hr; r.t., 2 hr

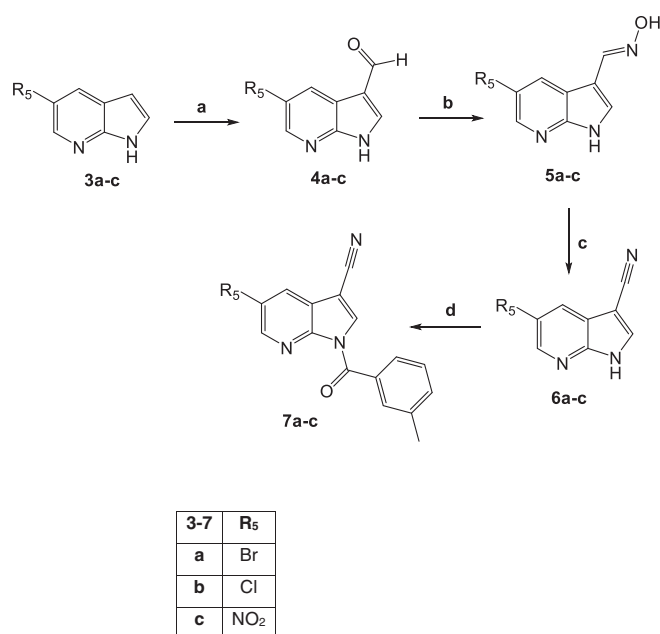


FIGURE 3 Reagents and conditions: (a) HTMA, CH₃COOH, reflux, 4 hr; (b) NH₂OH·HCl, H₂O, 60 °C, 30 min; NaHCO₃, reflux, 4 hr; (c) POCl₃, reflux, 1 hr; (d) *m*-Toluoyl chloride, NaH, dry THF, r.t., 24 hr

3-carbonitrile derivatives **6a-c** (6a, Graczyk, Palmer, & Khan, 2004), which were benzoylated at position 1 with *m*-toluoyl chloride and sodium hydride in anhydrous tetrahydrofuran to obtain the 5-substituted pyrrolo[2,3-*b*]pyridines **7a-c** (Figure 3).

Figure 4 shows the synthetic steps for insertion of (hetero)aromatic rings at position 5 to obtain final compounds **14a-g**. In the first step, the nitrogen at position 1 of intermediate **3a** (Joydev et al., 2017) was protected with benzensulfonyl chloride to obtain compound **8** (Liu et al., 2016), which subsequently was treated with tetrakis(triphenylphosphine)palladium(0), 2 M sodium carbonate solution, and the appropriate boronic acid in hot anhydrous toluene to obtain the corresponding 5-pyrrolo[2,3-*b*]pyridine derivatives **9a-g**. The protecting group at position N-1 was then removed with tetrabutylammonium fluoride (TBAF) in hot anhydrous tetrahydrofuran, resulting in pyrrolo[2,3-*b*]pyridines **10a-g** (10a, Laha et al., 2017; 10c and 10d, Ibrahim et al., 2007; 10f and 10g, Singh et al., 2017). Reaction of these compounds with hexamethylenetetramine (HMTA) in acetic acid at reflux resulted in the 3-formyl derivatives **11a-g** (11g, Ibrahim et al., 2007), which, when treated with hydroxylamine hydrochloride (**12a-g**), dehydrated with POCl₃ (**13a-g**), and benzoylated at position 1 with *m*-toluoyl chloride, led to final compounds **14a-g**.

2.2 | Experimental

All melting points were determined on a Büchi apparatus (New Castle, DE) and are uncorrected. Extracts were dried over Na₂SO₄, and the solvents were removed under reduced pressure. Merck F-254 commercial plates (Merck, Durham, NC) were used for analytical TLC to follow the course of reactions. Silica gel 60 (Merck 70–230 mesh, Merck, Durham, NC) was used for column chromatography. ¹H NMR

and ¹³C NMR spectra were recorded on an Avance 400 instrument (Bruker Biospin Version 002 with SGU, Bruker Inc., Billerica, MA). Chemical shifts (δ) are reported in ppm to the nearest 0.01 ppm using the solvent as an internal standard. Coupling constants (*J* values) are given in Hz and were calculated using TopSpin 1.3 software (Nicolet Instrument Corp., Madison, WI) and are rounded to the nearest 0.1 vHz. Mass spectra (*m/z*) were recorded on an ESI-TOF mass spectrometer (Bruker Micro TOF, Bruker Inc., Billerica, MA), and reported mass values are within the error limits of ±5 ppm mass units. Microanalyses indicated by the symbols of the elements were performed with a Perkin-Elmer 260 elemental analyzer (PerkinElmer, Inc., Waltham, MA) for C, H, and N, and the results were within ±0.4% of the theoretical values, unless otherwise stated. Reagents and starting materials were commercially available.

General procedure for compounds 2a-e. To a cooled (0 °C) suspension of the appropriate substrate **1a-e** (Bahekar et al., 2007; Baltus et al., 2016; Pires et al., 2016; Sandham et al., 2009) (0.56 mmol) in anhydrous CH₂Cl₂ (2 mL), 0.72 mmol of Et₃N, and 1.67 mmol of *m*-toluoyl chloride were added. The mixture was stirred at 0 °C for 2 hr and then at room temperature for an additional 2 hr. The solvent was evaporated, cold water was added, and the mixture was neutralized with 0.5 N NaOH. The reaction mixture was extracted with CH₂Cl₂ (3 × 15 mL), and the solvent was dried over sodium sulfate and evaporated in vacuum. The final compounds **2a-e** were purified by column chromatography using toluene/ethyl acetate 9.5:0.5 (for **2a,b**) or cyclohexane/ethyl acetate 2:1 (for **2c,d**) or 5:1 (for **2e**) as eluents.

(2-Methyl-1H-pyrrolo[2,3-*b*]pyridin-1-yl)(*m*-tolyl)methanone (2a). Yield = 67%; oil. ¹H-NMR (CDCl₃-d₁) δ 2.39 (s, 3H, *m*-CH₃-Ph), 2.56 (s, 3H, CH₃), 7.02–7.07 (m, 1H, Ar), 6.38 (s, 1H, Ar), 7.30 (t, 1H, Ar, *J* = 8.0 Hz), 7.41 (d, 1H, Ar, *J* = 8.0 Hz), 7.50 (d, 1H, Ar, *J* = 8.0 Hz), 7.66 (s, 1H, Ar), 7.76 (d, 1H, Ar, *J* = 8.0 Hz), 8.05 (d, 1H, Ar, *J* = 4.4 Hz). ¹³C-NMR (CDCl₃-d₁) δ 15.15 (CH₃), 21.33 (CH₃), 104.52 (CH), 117.37 (CH), 121.44 (C), 127.52 (CH), 128.04 (CH), 128.16 (CH), 131.13 (CH), 134.19 (CH), 134.77 (C), 138.16 (C), 138.90 (C), 142.62 (CH), 149.53 (C), 169.70 (CO). ESI-MS calcd. For C₁₆H₁₄N₂O, 250.30; found: *m/z* 251.11 [M+H]⁺. Anal. C₁₆H₁₄N₂O (C, H, N).

(2-Ethyl-1H-pyrrolo[2,3-*b*]pyridin-1-yl)(*m*-tolyl)methanone (2b). Yield = 17%; oil. ¹H-NMR (CDCl₃-d₁) δ 1.30 (t, 3H, CH₂CH₃, *J* = 7.2 Hz), 2.39 (s, 3H, *m*-CH₃-Ph), 2.98 (q, 2H, CH₂CH₃, *J* = 7.2 Hz), 6.43 (s, 1H, Ar), 7.03–7.08 (m, 1H, Ar), 7.30 (t, 1H, Ar, *J* = 7.6 Hz), 7.41 (d, 1H, Ar, *J* = 7.6 Hz), 7.49 (d, 1H, Ar, *J* = 7.6 Hz), 7.66 (s, 1H, Ar), 7.78 (d, 1H, Ar, *J* = 7.6 Hz), 8.05 (d, 1H, Ar, *J* = 4.4 Hz). ¹³C-NMR (CDCl₃-d₁) δ 12.82 (CH₃), 21.44 (CH₃), 21.81 (CH₂), 102.58 (CH), 118.02 (CH), 121.33 (C), 128.08 (CH), 129.30 (CH), 131.13 (CH), 134.29 (CH), 134.78 (C), 138.20 (C), 142.76 (CH), 145.09 (C), 149.74 (C), 169.93 (CO). ESI-MS calcd. For C₁₇H₁₆N₂O, 264.32; found: *m/z* 265.13 [M+H]⁺. Anal. C₁₇H₁₆N₂O (C, H, N).

Ethyl 1-(3-methylbenzoyl)-1H-pyrrolo[2,3-*b*]pyridine-2-carboxylate (2c). Yield = 34%; oil. ¹H-NMR (CDCl₃-d₁) δ 1.45 (t, 3H, OCH₂CH₃, *J* = 7.2 Hz), 2.38 (s, 3H, *m*-CH₃-Ph), 4.21 (q, 2H, OCH₂CH₃, *J* = 7.2 Hz), 7.16–7.21 (m, 1H, Ar), 7.29–7.34 (m, 2H, Ar), 7.42 (d, 1H, Ar, *J* = 7.6 Hz), 7.56 (d, 1H, Ar, *J* = 7.6 Hz), 7.71 (s, 1H, Ar), 8.04 (d, 1H, Ar, *J* = 8.0 Hz), 8.41 (d, 1H, Ar, *J* = 4.4 Hz). ¹³C-NMR (CDCl₃-d₁) δ 13.94 (CH₃), 21.29

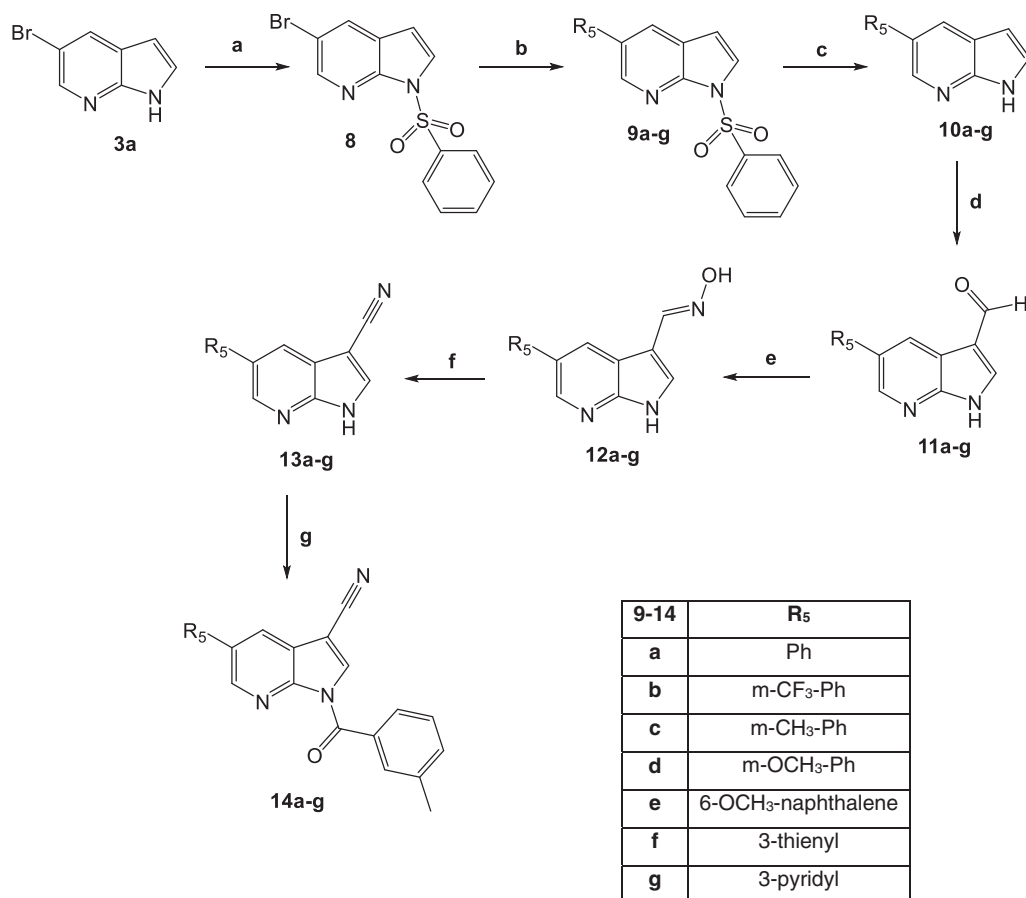


FIGURE 4 Reagents and conditions: (a) Ph-SO₂Cl, Et₃N, dry DCM, 0 °C, 2 hr then r.t., 2 hr; (b) R₅-B(OH)₂, Pd(PPh₃)₄, Na₂CO₃ 2 M, anhydrous toluene, reflux, 4–5 hr; (c) TBAF, dry THF, reflux, 2–6 hr; (d) HMTA, CH₃COOH, reflux, 6 hr; (e) NH₂OH·HCl, H₂O, 60 °C, 30 min; NaHCO₃, 100 °C, 4 hr; (f) POCl₃, reflux, 2 hr; (g) *m*-Toluoyl chloride, NaH, dry THF, r.t., 24 hr

(CH₃), 61.59 (CH₂), 111.04 (CH), 118.64 (CH), 119.46 (C), 127.93 (CH), 128.56 (CH), 130.65 (C), 131.02 (CH), 131.18 (CH), 134.03 (C), 135.01 (CH), 138.61 (C), 147.70 (CH), 150.05 (C), 160.65 (C), 169.00 (CO). ESI-MS calcd. For C₁₈H₁₆N₂O₃, 308.34; found: *m/z* 309.12 [M+H]⁺. Anal. C₁₈H₁₆N₂O₃ (C, H, N).

1-(3-Methylbenzoyl)-1H-pyrrolo[2,3-b]pyridine-2-carbonitrile (2d). Yield = 41%; oil. ¹H-NMR (CDCl₃-d₁) δ 2.41 (s, 3H, m-CH₃-Ph), 7.25–7.33 (m, 1H, Ar), 7.34–7.40 (m, 2H, Ar), 7.48 (d, 1H, Ar, *J* = 7.6 Hz), 7.58 (d, 1H, Ar, *J* = 7.6 Hz) 7.69 (s, 1H, Ar), 8.03 (dd, 1H, Ar, *J* = 8.0 Hz and *J* = 1.2 Hz), 8.38 (d, 1H, Ar, *J* = 3.6 Hz). ¹³C-NMR (CDCl₃-d₁) δ 21.53 (CH₃), 110.31 (C), 112.22 (C), 118.23 (CH), 119.60 (C), 120.03 (CH), 128.32 (CH), 128.59 (CH), 131.13 (CH), 131.61 (CH), 132.56 (C), 135.23 (CH), 138.52 (C), 148.37 (CH), 166.85 (CO). ESI-MS calcd. For C₁₆H₁₁N₃O, 261.28; found: *m/z* 262.09 [M+H]⁺. Anal. C₁₆H₁₁N₃O (C, H, N).

2-Methyl-1-(3-methylbenzoyl)-1H-pyrrolo[2,3-b]pyridine-3-carbonitrile (2e). Yield = 10%; oil. ¹H-NMR (CDCl₃-d₁) δ 2.40 (s, 3H, m-CH₃-Ph), 2.74 (s, 3H, CH₃), 7.21–7.26 (m, 1H, Ar), 7.35 (d, 1H, Ar), 7.48 (d, 2H, Ar, *J* = 7.6 Hz), 7.64 (s, 1H, Ar), 7.98 (d, 1H, Ar, *J* = 7.2 Hz), 8.19 (d, 1H, Ar, *J* = 4.0 Hz). ¹³C-NMR (CDCl₃-d₁) δ 9.43 (CH₃), 20.91 (CH₃), 101.37 (C), 115.65 (CH), 115.92 (C), 121.15 (CH), 128.10 (CH), 128.36 (CH), 129.14 (CH), 130.17 (CH), 130.49 (CH), 134.86 (CH), 137.33 (C),

138.91 (C), 142.4 (CH), 146.36 (C), 167.70 (CO). ESI-MS calcd. For C₁₇H₁₃N₃O, 275.30; found: *m/z* 276.11 [M+H]⁺. Anal. C₁₇H₁₃N₃O (C, H, N).

General procedure for compounds 5a and 5c. A mixture of the appropriate 1H-pyrrolo[2,3-b]pyridine-3-carbaldehyde **4a** (Xi & Li, 2014) or **4c** (Ermoli et al., 2009) (0.78 mmol) and hydroxylamine hydrochloride (2.35 mmol) in 2 mL of water was heated at 60 °C for 30 min. NaHCO₃ (2.35 mmol) was then added, and the reaction mixture was heated under reflux for 4 hr at 100 °C. After cooling at room temperature, the solid was filtered, washed with the excess of ice-cold water and dried. The crude product was recrystallized from hexane to obtain the pure product.

(E)-5-Bromo-1H-pyrrolo[2,3-b]pyridine-3-carbaldehyde oxime (5a). Yield = 94%; mp = 235–237 °C (hexane). ¹H-NMR (DMSO-d₆) δ 7.81 (s, 1H, CH=N-OH), 8.21 (s, 1H, Ar), 8.33 (s, 1H, Ar), 8.38 (s, 1H, Ar), 10.75 (exch br s, 1H, CH=N-OH), 12.16 (exch br s, 1H, NH). ESI-MS calcd. For C₈H₆BrN₃O, 240.06; found: *m/z* 240.97 [M+H]⁺. Anal. C₈H₆BrN₃O (C, H, N).

(E)-5-nitro-1H-pyrrolo[2,3-b]pyridine-3-carbaldehyde oxime (5c). Yield = 40%; mp = 193–195 °C (hexane). ¹H-NMR (DMSO-d₆) δ 8.00 (s, 1H, Ar), 8.27 (s, 1H, CH=N-OH), 9.04 (s, 1H, Ar), 9.13 (s, 1H, Ar), 11.02 (exch br s, 1H, CH=N-OH), 12.70 (exch br s, 1H, NH). ESI-MS

calcd. For $C_8H_6N_4O_3$, 206.16; found: m/z 207.05 $[M+H]^+$. Anal. $C_8H_6N_4O_3$ (C, H, N).

General procedure for compounds 6b and 6c. A suspension of intermediate **5b** (Bahekar et al., 2007) or **5c** (0.92 mmol) in 4 mL of $POCl_3$ was stirred at reflux for 2 hr. After cooling, ice-cold water (20 mL) was slowly added, and the precipitate was filtered under vacuum and washed with abundant cold water to obtain the desired compound, which was recrystallized from ethanol.

5-Chloro-1H-pyrrolo[2,3-b]pyridine-3-carbonitrile (6b). Yield = 90%; mp = 291–294 °C (EtOH). 1H -NMR (DMSO- d_6) δ 8.27 (d, 1H, Ar, J = 2.0 Hz), 8.40 (d, 1H, Ar, J = 2.4 Hz), 8.51 (d, 1H, Ar, J = 3.2 Hz), 13.05 (exch br s, 1H, NH). IR ν (cm^{-1}): 2240 (CN). ESI-MS calcd. For $C_8H_4ClN_3$, 177.59; found: m/z 179.01 $[M+H]^+$. Anal. $C_8H_4ClN_3$ (C, H, N).

5-Nitro-1H-pyrrolo[2,3-b]pyridine-3-carbonitrile (6c). Yield = 81%; mp = 248–250 °C (EtOH). 1H -NMR (DMSO- d_6) δ 8.71 (s, 1H, Ar), 8.91 (s, 1H, Ar), 9.21 (s, 1H, Ar), 13.56 (exch br s, 1H, NH). IR ν (cm^{-1}): 2220 (CN). ESI-MS calcd. For $C_8H_4N_4O_2$, 188.14; found: m/z 189.04 $[M+H]^+$. Anal. $C_8H_4N_4O_2$ (C, H, N).

General procedure for compounds 7a-c. To a suspension of the substrate **6a-c** (**6a**, Graczyk et al., 2004) (0.53 mmol) in 10 mL of anhydrous THF, 1.06 mmol of sodium hydride and 0.64 mmol of *m*-toluoyl chloride were added. The mixture was stirred at room temperature overnight. The solvent was concentrated in vacuo to obtain a residue that was purified by column chromatography using cyclohexane/ethyl acetate 6:1 (for **7a,b**) or 5:1 (for **7c**) as eluents.

5-Bromo-1-(3-methylbenzoyl)-1H-pyrrolo[2,3-b]pyridine-3-carbonitrile (7a). Yield = 30%; mp = 156–159 °C (EtOH). 1H -NMR ($CDCl_3$ - d_1) δ 2.44 (s, 3H, *m*-CH₃-Ph), 7.41 (t, 1H, Ar, J = 7.6 Hz), 7.50–7.55 (m, 2H, Ar), 7.62 (s, 1H, Ar), 8.20–8.25 (m, 2H, Ar), 8.46 (s, 1H, Ar). ^{13}C -NMR ($CDCl_3$ - d_1) δ 21.52 (CH₃), 90.31 (C), 127.78 (CH), 128.67 (CH), 131.11 (CH), 131.77 (C), 135.21 (CH), 136.23 (CH), 138.87 (C), 145.41 (C), 166.46 (CO). IR ν (cm^{-1}): 2224 (CN). ESI-MS calcd. For $C_{16}H_{10}BrN_3O$, 340.17; found: m/z 341.00 $[M+H]^+$. Anal. $C_{16}H_{10}BrN_3O$ (C, H, N).

5-Chloro-1-(3-methylbenzoyl)-1H-pyrrolo[2,3-b]pyridine-3-carbonitrile (7b). Yield = 10%; mp = 150–152 °C (EtOH). 1H -NMR ($CDCl_3$ - d_1) δ 2.44 (s, 3H, *m*-CH₃-Ph), 7.41 (t, 1H, Ar, J = 7.2 Hz), 7.50–7.55 (m, 2H, Ar), 7.62 (s, 1H, Ar), 8.10 (s, 1H, Ar), 8.24 (s, 1H, Ar), 8.38 (s, 1H, Ar). ^{13}C -NMR ($CDCl_3$ - d_1) δ 21.32 (CH₃), 112.77 (C), 127.79 (CH), 127.96 (CH), 128.48 (CH), 128.71 (C), 130.99 (CH), 131.01 (C), 135.06 (CH), 136.04 (CH), 138.82 (C), 145.11 (C), 145.63 (CH), 166.33 (CO). IR ν (cm^{-1}): 2223 (CN). ESI-MS calcd. For $C_{16}H_{10}ClN_3O$, 295.72; found: m/z 297.05 $[M+H]^+$. Anal. $C_{16}H_{10}ClN_3O$ (C, H, N).

1-(3-Methylbenzoyl)-5-nitro-1H-pyrrolo[2,3-b]pyridine-3-carbonitrile (7c). Yield = 35%; mp = 152–154 °C (EtOH). 1H -NMR ($CDCl_3$ - d_1) δ 2.45 (s, 3H, *m*-CH₃-Ph), 7.43 (t, 1H, Ar, J = 7.6 Hz), 7.55 (d, 2H, Ar, J = 7.6 Hz), 7.64 (s, 1H, Ar), 8.43 (s, 1H, Ar), 8.96 (d, 1H, Ar, J = 2.4 Hz), 9.27 (d, 1H, Ar, J = 2.4 Hz). ^{13}C -NMR ($CDCl_3$ - d_1) δ 20.93 (CH₃), 101.34 (C), 115.51 (C), 122.13 (C), 123.68 (CH), 128.16 (CH), 129.19 (CH), 130.42 (C), 130.57 (CH), 131.62 (C), 134.11 (CH), 137.65 (CH), 138.94 (C), 152.78 (C), 167.74 (CO). IR ν (cm^{-1}): 2220 (CN). ESI-MS calcd. For $C_{16}H_{10}N_4O_3$, 306.28; found: m/z 307.08 $[M+H]^+$. Anal. $C_{16}H_{10}N_4O_3$ (C, H, N).

General procedure for compounds 9a-g. To a suspension of intermediate **8** (Liu et al., 2016) (0.34 mmol) in 3 mL of toluene, 0.051 mmol of tetrakis(triphenylphosphine)palladium(0), 3 mL of Na_2CO_3 2 M solution, and 0.68 mmol of the appropriate hetero(phenyl)-boronic acid were added. The mixture was stirred at reflux for 4 hr. After cooling, ice-cold water (20 mL) was added, the suspension was extracted with CH_2Cl_2 (3 \times 15 mL), dried over sodium sulfate, and the solvent was evaporated in vacuo to obtain compounds **9a-g**, which were purified by column chromatography using hexane/ethyl acetate 3:1 (for **9b,e**), hexane/acetone 4:1 (for **9a,c,d,f**), or cyclohexane/ethyl acetate 1:5 (for **9g**) as eluents.

5-Phenyl-1-(phenylsulfonyl)-1H-pyrrolo[2,3-b]pyridine (9a). Yield = 79%; mp = 123–125 °C (EtOH). 1H -NMR ($CDCl_3$ - d_1) δ 6.63 (d, 1H, Ar, J = 4.0 Hz), 7.36 (t, 1H, Ar, J = 7.2 Hz), 7.42–7.49 (m, 4H, Ar), 7.52–7.57 (m, 3H, Ar), 7.75 (d, 1H, Ar, J = 4.0 Hz), 7.98 (d, 1H, Ar, J = 2.0 Hz), 8.22 (d, 2H, Ar, J = 7.2 Hz), 8.65 (d, 1H, Ar, J = 2.0 Hz). ESI-MS calcd. For $C_{19}H_{14}N_2O_2S$, 334.39; found: m/z 335.08 $[M+H]^+$. Anal. $C_{19}H_{14}N_2O_2S$ (C, H, N).

1-(Phenylsulfonyl)-5-(3-(trifluoromethyl)phenyl)-1H-pyrrolo[2,3-b]pyridine (9b). Yield = 79%; mp = 145–148 °C (EtOH). 1H -NMR ($CDCl_3$ - d_1) δ 6.66 (d, 1H, Ar, J = 4.0 Hz), 7.50 (t, 2H, Ar, J = 8.0 Hz), 7.56–7.61 (m, 2H, Ar), 7.63 (d, 1H, Ar, J = 7.6 Hz), 7.72 (d, 1H, Ar, J = 7.6 Hz), 7.78 (d, 2H, Ar, J = 4.0 Hz), 8.02 (d, 1H, Ar, J = 2.0 Hz), 8.22 (d, 2H, Ar, J = 7.2 Hz), 8.63 (d, 1H, Ar, J = 2.0 Hz). ESI-MS calcd. For $C_{20}H_{13}F_3N_2O_2S$, 402.39; found: m/z 403.07 $[M+H]^+$. Anal. $C_{20}H_{13}F_3N_2O_2S$ (C, H, N).

1-(Phenylsulfonyl)-5-(*m*-tolyl)-1H-pyrrolo[2,3-b]pyridine (9c). Yield = 78%; mp = 140–143 °C (EtOH). 1H -NMR ($CDCl_3$ - d_1) δ 2.41 (s, 3H, *m*-CH₃-Ph), 6.63 (d, 1H, Ar, J = 4.0 Hz), 7.19 (s, 1H, Ar), 7.30–7.35 (m, 3H, Ar), 7.48 (t, 1H, Ar, J = 8.0 Hz), 7.56 (t, 2H, Ar, J = 7.6 Hz), 7.75 (d, 1H, Ar, J = 4.0 Hz), 7.98 (d, 1H, Ar, J = 2.0 Hz), 8.22 (d, 2H, Ar, J = 7.6 Hz), 8.64 (d, 1H, Ar, J = 2.0 Hz). ESI-MS calcd. For $C_{20}H_{16}N_2O_2S$, 348.42; found: m/z 349.10 $[M+H]^+$. Anal. $C_{20}H_{16}N_2O_2S$ (C, H, N).

5-(3-Methoxyphenyl)-1-(phenylsulfonyl)-1H-pyrrolo[2,3-b]pyridine (9d). Yield = 78%; mp = 106–109 °C (EtOH). 1H -NMR ($CDCl_3$ - d_1) δ 3.85 (s, 3H, OCH₃), 6.64 (d, 1H, Ar, J = 4.0 Hz), 6.92 (dd, 1H, Ar, J = 2.0 Hz and J = 8.4 Hz), 7.07 (s, 1H, Ar), 7.12 (d, 1H, Ar, J = 7.6 Hz), 7.37 (t, 1H, Ar, J = 7.6 Hz), 7.50 (t, 2H, Ar, J = 8.0 Hz), 7.58 (t, 1H, Ar, J = 7.6 Hz), 7.75 (d, 1H, Ar, J = 4.0 Hz), 8.00 (d, 1H, Ar, J = 2.0 Hz), 8.22 (d, 2H, Ar, J = 7.6 Hz), 8.65 (d, 1H, Ar, J = 2.0 Hz). ESI-MS calcd. For $C_{20}H_{16}N_2O_3S$, 364.42; found: m/z 365.09 $[M+H]^+$. Anal. $C_{20}H_{16}N_2O_3S$ (C, H, N).

5-(6-Methoxynaphthalen-2-yl)-1-(phenylsulfonyl)-1H-pyrrolo[2,3-b]pyridine (9e). Yield = 91%; mp = 173–176 °C (EtOH) dec. 1H -NMR ($CDCl_3$ - d_1) δ 3.93 (s, 3H, OCH₃), 6.65 (d, 1H, Ar, J = 3.6 Hz), 7.15–7.21 (m, 2H, Ar), 7.49 (t, 2H, Ar, J = 8.0 Hz), 7.56 (d, 1H, Ar, J = 7.2 Hz), 7.64 (d, 1H, Ar, J = 8.0 Hz), 7.75–7.83 (m, 3H, Ar), 7.92 (s, 1H, Ar), 8.08 (s, 1H, Ar), 8.24 (d, 2H, Ar, J = 7.6 Hz), 8.75 (s, 1H, Ar). ESI-MS calcd. For $C_{24}H_{18}N_2O_3S$, 414.48; found: m/z 415.11 $[M+H]^+$. Anal. $C_{24}H_{18}N_2O_3S$ (C, H, N).

1-(Phenylsulfonyl)-5-(thiophen-3-yl)-1H-pyrrolo[2,3-b]pyridine (9f). Yield = 55%; mp = 186–189 °C (EtOH). 1H -NMR ($CDCl_3$ - d_1) δ

6.59–6.63 (m, 1H, Ar), 7.22–7.27 (m, 1H, Ar), 7.35–7.50 (m, 4H, Ar), 7.53–7.58 (m, 1H, Ar), 7.70–7.75 (m, 1H, Ar), 8.00 (s, 1H, Ar), 8.18–8.23 (m, 2H, Ar), 8.68 (s, 1H, Ar). ESI-MS calcd. For $C_{17}H_{12}N_2O_2S_2$, 340.43; found: m/z 341.04 [M+H]⁺. Anal. $C_{17}H_{12}N_2O_2S_2$ (C, H, N).

1-(Phenylsulfonyl)-5-(pyridin-3-yl)-1H-pyrrolo[2,3-b]pyridine (9g). Yield = 98%; mp = 148–152 °C (EtOH). ¹H-NMR (CDCl₃-d₁) δ 6.68 (d, 1H, Ar, *J* = 3.6 Hz), 7.49–7.62 (m, 4H, Ar), 7.82 (s, 1H, Ar), 8.03 (s, 2H, Ar), 8.23 (d, 2H, Ar, *J* = 7.6 Hz), 8.62–8.67 (m, 2H, Ar), 8.85 (s, 1H, Ar). ESI-MS calcd. For $C_{18}H_{13}N_3O_2S$, 335.38; found: m/z 336.08 [M+H]⁺. Anal. $C_{18}H_{13}N_3O_2S$ (C, H, N).

General procedure for compounds 10b and 10e. To a solution of intermediate **9b** or **9e** (0.29 mmol) in anhydrous THF (3 mL), 0.87 mmol of TBAF was added, and the mixture was stirred at reflux for 4 hr. After cooling, the solvent was evaporated, and cold-ice water (20 mL) was added. The precipitate was recovered by vacuum filtration and purified by crystallization from ethanol to obtain the desired compound **10b** or by column chromatography using cyclohexane/ethyl acetate 1:1 as eluent for **10e**.

5-(3-[Trifluoromethyl]phenyl)-1H-pyrrolo[2,3-b]pyridine (10b). Yield = 97%; mp = 158–161 °C (EtOH). ¹H-NMR (CDCl₃-d₁) δ 6.65 (d, 1H, Ar, *J* = 3.2 Hz), 7.47 (d, 1H, Ar, *J* = 3.2 Hz), 7.59–7.67 (m, 2H, Ar), 7.80 (d, 1H, Ar, *J* = 7.2 Hz), 7.86 (s, 1H, Ar), 8.27 (d, 1H, Ar, *J* = 1.2 Hz), 8.54 (s, 1H, Ar), 10.12 (exch br s, 1H, NH). ESI-MS calcd. For $C_{14}H_9F_3N_2$, 262.23; found: m/z 263.08 [M+H]⁺. Anal. $C_{14}H_9F_3N_2$ (C, H, N).

5-(6-Methoxynaphthalen-2-yl)-1H-pyrrolo[2,3-b]pyridine (10e). Yield = 45%; mp = 247–250 °C dec (EtOH). ¹H-NMR (CDCl₃-d₁) δ 3.87 (s, 3H, OCH₃), 6.50 (d, 1H, Ar, *J* = 1.6 Hz), 7.18 (dd, 1H, Ar, *J* = 2.4 Hz and *J* = 8.4 Hz), 7.33 (s, 1H, Ar), 7.50 (d, 1H, Ar, *J* = 2.4 Hz), 7.82–7.90 (m, 3H, Ar), 8.16 (d, 1H, Ar, *J* = 4.0 Hz), 8.29 (d, 1H, Ar, *J* = 3.6 Hz), 8.62 (d, 1H, Ar, *J* = 3.2 Hz), 11.71 (exch br s, 1H, NH). ESI-MS calcd. For $C_{18}H_{14}N_2O$, 274.32; found: m/z 275.11 [M+H]⁺. Anal. $C_{18}H_{14}N_2O$ (C, H, N).

General procedure for compounds 11a-f. A mixture of the appropriate 1H-pyrrolo[2,3-b]pyridine derivative **10a-f** (0.95 mmol) (**10a**, Laha et al., 2017; **10c** and **10d**, Ibrahim et al., 2007; **10f**, Singh et al., 2017) and HMTA (1.43 mmol) in glacial acetic acid (3 mL) was heated under reflux for 6 hr. The reaction mixture was cooled at room temperature and diluted with cold water. The solid obtained was filtered, washed with an excess of ice-cold water, and dried. The crude compound was purified by crystallization from hexane (**11b,e**) or by column chromatography using cyclohexane/ethyl acetate 1:3 (for **11a,d**), dichloromethane/methanol 95:5 (for **11c**), or cyclohexane/ethyl acetate 1:5 (for **11f**) as eluents.

5-Phenyl-1H-pyrrolo[2,3-b]pyridine-3-carbaldehyde (11a). Yield = 56%; mp = 212–215 °C (EtOH). ¹H-NMR (CDCl₃-d₁) δ 7.42 (t, 1H, Ar, *J* = 7.2 Hz), 7.51 (t, 2H, Ar, *J* = 7.6 Hz), 7.67 (d, 2H, Ar, *J* = 7.2 Hz), 8.10 (s, 1H, Ar), 8.68 (s, 1H, Ar), 8.89 (s, 1H, Ar), 10.08 (s, 1H, CHO), 11.82 (exch br s, 1H, NH). ESI-MS calcd. For $C_{14}H_{10}N_2O$, 222.24; found: m/z 223.08 [M+H]⁺. Anal. $C_{14}H_{10}N_2O$ (C, H, N).

5-(3-[Trifluoromethyl]phenyl)-1H-pyrrolo[2,3-b]pyridine-3-carbaldehyde (11b). Yield = 80%; mp = 193–196 °C (hexane). ¹H-NMR (DMSO-d₆) δ 7.23 (d, 2H, Ar, *J* = 7.2 Hz), 8.04 (d, 2H, Ar, *J* = 8.4 Hz),

8.52 (s, 1H, Ar), 8.63 (d, 1H, Ar, *J* = 2.0 Hz), 8.71 (d, 1H, Ar, *J* = 2.0 Hz), 9.45 (s, 1H, CHO), 12.65 (exch br s, 1H, NH). ESI-MS calcd. For $C_{15}H_9F_3N_2O$, 290.24; found: m/z 291.07 [M+H]⁺. Anal. $C_{15}H_9F_3N_2O$ (C, H, N).

5-(m-Tolyl)-1H-pyrrolo[2,3-b]pyridine-3-carbaldehyde (11c). Yield = 62%; mp = 162–165 °C (EtOH). ¹H-NMR (DMSO-d₆) δ 2.38 (s, 3H, CH₃), 7.19 (d, 1H, Ar, *J* = 7.6 Hz), 7.36 (t, 1H, Ar, *J* = 7.2 Hz), 7.48 (d, 1H, Ar, *J* = 7.6 Hz), 7.52 (s, 1H, Ar), 8.48 (s, 1H, Ar), 8.55 (d, 1H, Ar, *J* = 2.0 Hz), 8.62 (d, 1H, Ar, *J* = 2.0 Hz), 9.93 (s, 1H, CHO), 12.75 (exch br s, 1H, NH). ESI-MS calcd. For $C_{15}H_{12}N_2O$, 236.27; found: m/z 237.10 [M+H]⁺. Anal. $C_{15}H_{12}N_2O$ (C, H, N).

5-(3-Methoxyphenyl)-1H-pyrrolo[2,3-b]pyridine-3-carbaldehyde (11d). Yield = 37%; mp = 200–203 °C (EtOH). ¹H-NMR (DMSO-d₆) δ 3.90 (s, 3H, OCH₃), 6.97 (d, 1H, Ar, *J* = 8.4 Hz), 7.17 (s, 1H, Ar), 7.23 (s, 1H, Ar), 7.42 (t, 1H, Ar, *J* = 8.0 Hz), 8.07 (s, 1H, Ar), 8.64 (s, 1H, Ar), 8.92 (s, 1H, Ar), 10.08 (s, 1H, CHO), 12.70 (exch br s, 1H, NH). ESI-MS calcd. For $C_{15}H_{12}N_2O_2$, 252.27; found: m/z 253.09 [M+H]⁺. Anal. $C_{15}H_{12}N_2O_2$ (C, H, N).

5-(6-Methoxynaphthalen-2-yl)-1H-pyrrolo[2,3-b]pyridine-3-carbaldehyde (11e). Yield = 84%; mp = 145–147 °C (hexane). ¹H-NMR (DMSO-d₆) δ 3.88 (s, 3H, OCH₃), 7.20 (d, 1H, Ar, *J* = 8.8 Hz), 7.36 (s, 1H, Ar), 7.84–7.95 (m, 3H, Ar), 8.21 (s, 1H, Ar), 8.52 (s, 1H, Ar), 8.69 (s, 1H, Ar), 8.78 (s, 1H, Ar), 9.97 (s, 1H, CHO), 12.57 (exch br s, 1H, NH). ESI-MS calcd. For $C_{19}H_{14}N_2O_2$, 302.33; found: m/z 303.11 [M+H]⁺. Anal. $C_{19}H_{14}N_2O_2$ (C, H, N).

5-(Thiophen-3-yl)-1H-pyrrolo[2,3-b]pyridine-3-carbaldehyde (11f). Yield = 37%; mp = 194–196 °C (EtOH). ¹H-NMR (DMSO-d₆) δ 7.60–7.66 (m, 2H, Ar), 7.95 (s, 1H, Ar), 8.46 (s, 1H, Ar), 8.60 (s, 1H, Ar), 8.74 (s, 1H, Ar), 9.93 (s, 1H, CHO), 12.71 (exch br s, 1H, NH). ESI-MS calcd. For $C_{12}H_8N_2OS$, 228.27; found: m/z 229.04 [M+H]⁺. Anal. $C_{12}H_8N_2OS$ (C, H, N).

General procedure for compounds 12a-g. Compounds **12a-g** were obtained following the same procedure reported for compounds **5a,c**, but starting with intermediates **11a-g** (**11g**, Ibrahim et al., 2007). The crude products were purified by crystallization from ethanol (**12c,d,g**) or by column chromatography using cyclohexane/ethyl acetate 1:5 (for **12a,b**), cyclohexane/ethyl acetate 1:2 (for **12e**), or cyclohexane/ethyl acetate 1:3 (for **12f**) as eluents.

5-Phenyl-1H-pyrrolo[2,3-b]pyridine-3-carbaldehyde oxime (12a). Yield = 42%; mp = 224–226 °C (EtOH). ¹H-NMR (CDCl₃-d₁) δ 7.40 (d, 1H, Ar, *J* = 7.6 Hz), 7.46–7.52 (m, 3H, 2H Ar + 1H CH=N-OH), 7.63 (d, 2H, Ar, *J* = 7.6 Hz), 8.33 (s, 1H, Ar), 8.59 (s, 1H, Ar), 8.69 (s, 1H, Ar), 10.31 (exch br s, 1H, CH=N-OH), 11.95 (exch br s, 1H, NH). ESI-MS calcd. For $C_{14}H_{11}N_3O$, 237.26; found: m/z 238.09 [M+H]⁺. Anal. $C_{14}H_{11}N_3O$ (C, H, N).

5-(3-[Trifluoromethyl]phenyl)-1H-pyrrolo[2,3-b]pyridine-3-carbaldehyde oxime (12b). Yield = 52%; mp = 247–250 °C (EtOH). ¹H-NMR (DMSO-d₆) δ 7.72 (d, 3H, Ar, *J* = 4.0 Hz), 7.82 (s, 1H, CH=N-OH), 7.96 (s, 1H, Ar), 8.28 (s, 1H, Ar), 8.51 (d, 1H, Ar, *J* = 2.0 Hz), 8.64 (d, 1H, Ar, *J* = 1.6 Hz), 10.74 (exch br s, 1H, CH=N-OH), 12.10 (exch br s, 1H, NH). ESI-MS calcd. For $C_{15}H_{10}F_3N_3O$, 305.25; found: m/z 306.08 [M+H]⁺. Anal. $C_{15}H_{10}F_3N_3O$ (C, H, N).

5-(m-Tolyl)-1H-pyrrolo[2,3-b]pyridine-3-carbaldehyde oxime (12c). Yield = 51%; mp = 208–211 °C (EtOH). $^1\text{H-NMR}$ (DMSO- d_6) δ 2.37 (s, 3H, CH₃), 7.16 (s, 1H, CH=N-OH), 7.35 (t, 1H, Ar, J = 7.6 Hz), 7.44 (t, 1H, Ar, J = 7.6 Hz), 7.50–7.56 (m, 1H, Ar), 7.78 (d, 1H, Ar, J = 2.0 Hz), 8.25–8.30 (m, 1H, Ar), 8.46 (d, 1H, Ar, J = 2.0 Hz), 8.54–8.59 (m, 1H, Ar), 10.71 (exch br s, 1H, CH=N-OH), 12.00 (exch br s, 1H, NH). ESI-MS calcd. For C₁₅H₁₃N₃O, 251.28; found: m/z 252.11 [M+H]⁺. Anal. C₁₅H₁₃N₃O (C, H, N).

5-(3-Methoxyphenyl)-1H-pyrrolo[2,3-b]pyridine-3-carbaldehyde oxime (12d). Yield = 84%; mp = 191–194 °C (EtOH). $^1\text{H-NMR}$ (DMSO- d_6) δ 3.81 (s, 3H, OCH₃), 6.91–6.96 (m, 1H, Ar), 7.17–7.22 (m, 2H, Ar), 7.35–7.40 (m, 2H, 1H Ar + 1H CH=N-OH), 7.78 (s, 1H, Ar), 8.26 (s, 1H, Ar), 8.64 (s, 1H, Ar), 10.72 (exch br s, 1H, CH=N-OH), 12.03 (exch br s, 1H, NH). ESI-MS calcd. For C₁₅H₁₃N₃O₂, 267.28; found: m/z 268.10 [M+H]⁺. Anal. C₁₅H₁₃N₃O₂ (C, H, N).

5-(6-Methoxynaphthalen-2-yl)-1H-pyrrolo[2,3-b]pyridine-3-carbaldehyde oxime (12e). Yield = 37%; mp = 204–207 °C dec (EtOH). $^1\text{H-NMR}$ (DMSO- d_6) δ 3.88 (s, 3H, OCH₃), 7.19 (d, 1H, Ar, J = 8.4 Hz), 7.35 (s, 1H, Ar), 7.74–7.79 (m, 1H, Ar), 7.89–7.94 (m, 3H, Ar), 8.12 (s, 1H, CH=N-OH), 8.29 (d, 1H, Ar, J = 6.8 Hz), 8.57 (s, 1H, Ar), 8.66–8.71 (m, 1H, Ar), 10.73 (exch br s, 1H, CH=N-OH), 12.01 (exch br s, 1H, NH). ESI-MS calcd. For C₁₉H₁₅N₃O₂, 317.34; found: m/z 318.12 [M+H]⁺. Anal. C₁₉H₁₅N₃O₂ (C, H, N).

5-(Thiophen-3-yl)-1H-pyrrolo[2,3-b]pyridine-3-carbaldehyde oxime (12f). Yield = 54%; mp = 239–242 °C (EtOH). $^1\text{H-NMR}$ (DMSO- d_6) δ 7.50 (d, 1H, Ar, J = 4.8 Hz), 7.66 (s, 1H, Ar), 7.77 (d, 1H, Ar, J = 7.6 Hz), 8.25 (s, 1H, CH=N-OH), 8.45 (s, 1H, Ar), 8.62–8.67 (m, 2H, Ar), 10.71 (exch br s, 1H, CH=N-OH), 11.99 (exch br s, 1H, NH). ESI-MS calcd. For C₁₂H₉N₃OS, 243.28; found: m/z 244.05 [M+H]⁺. Anal. C₁₂H₉N₃OS (C, H, N).

5-(Pyridin-3-yl)-1H-pyrrolo[2,3-b]pyridine-3-carbaldehyde oxime (12g). Yield = 67%; mp = 241–243 °C (EtOH). $^1\text{H-NMR}$ (DMSO- d_6) δ 7.50 (d, 1H, Ar, J = 4.8 Hz), 7.79 (s, 1H, Ar), 8.07 (d, 1H, Ar, J = 6.4 Hz), 8.27 (s, 1H, CH=N-OH), 8.49–8.65 (m, 3H, Ar), 8.81 (s, 1H, Ar), 10.74 (exch br s, 1H, CH=N-OH), 12.10 (exch br s, 1H, NH). ESI-MS calcd. For C₁₃H₁₀N₄O, 238.24; found: m/z 239.09 [M+H]⁺. Anal. C₁₃H₁₀N₄O (C, H, N).

General procedure for compounds 13a–g. Compounds 13a–g were obtained following the same procedure reported for compounds 6b,c, but starting with intermediates 12a–g. The crude products were purified by crystallization from ethanol.

5-Phenyl-1H-pyrrolo[2,3-b]pyridine-3-carbonitrile (13a). Yield = 40%; mp = 199–202 °C (EtOH). $^1\text{H-NMR}$ (CDCl₃- d_1) δ 7.47 (d, 1H, Ar, J = 7.2 Hz), 7.53 (t, 2H, Ar, J = 7.2 Hz), 7.63 (d, 2H, Ar, J = 7.6 Hz), 7.97 (s, 1H, Ar), 8.48 (s, 1H, Ar), 8.71 (s, 1H, Ar), 12.65 (exch br s, 1H, NH). IR ν (cm⁻¹): 2220 (CN). ESI-MS calcd. For C₁₄H₉N₃, 219.24; found: m/z 220.08 [M+H]⁺. Anal. C₁₄H₉N₃ (C, H, N).

5-(3-[Trifluoromethyl]phenyl)-1H-pyrrolo[2,3-b]pyridine-3-carbonitrile (13b). Yield = 85%; mp = 240–242 °C (EtOH). $^1\text{H-NMR}$ (CDCl₃- d_1) δ 7.70 (t, 1H, Ar, J = 7.6 Hz), 7.76 (d, 1H, Ar, J = 7.6 Hz), 7.82 (d, 1H, Ar, J = 7.6 Hz), 7.88 (s, 1H, Ar), 8.09 (s, 1H, Ar), 8.62 (s, 1H, Ar), 8.71 (s, 1H, Ar), 12.75 (exch br s, 1H, NH). IR ν (cm⁻¹): 2222 (CN). ESI-MS calcd. For C₁₅H₈F₃N₃, 287.24; found: m/z 288.07 [M+H]⁺. Anal. C₁₅H₈F₃N₃ (C, H, N).

5-(m-Tolyl)-1H-pyrrolo[2,3-b]pyridine-3-carbonitrile (13c). Yield = 74%; mp = 194–197 °C (EtOH). $^1\text{H-NMR}$ (DMSO- d_6) δ 2.38 (s, 3H, CH₃), 7.19 (d, 1H, Ar, J = 7.6 Hz), 7.36 (t, 1H, Ar, J = 7.6 Hz), 7.55 (d, 1H, Ar, J = 7.6 Hz), 7.61 (s, 1H, Ar), 8.29 (d, 1H, Ar, J = 1.6 Hz), 8.46 (d, 1H, Ar, J = 2.4 Hz), 8.67 (d, 1H, Ar, J = 2.0 Hz), 12.87 (exch br s, 1H, NH). IR ν (cm⁻¹): 2220 (CN). ESI-MS calcd. For C₁₅H₁₁N₃, 233.27; found: m/z 234.10 [M+H]⁺. Anal. C₁₅H₁₁N₃ (C, H, N).

5-(3-Methoxyphenyl)-1H-pyrrolo[2,3-b]pyridine-3-carbonitrile (13d). Yield = 94%; mp = 201–204 °C (EtOH). $^1\text{H-NMR}$ (CDCl₃- d_1) δ 3.83 (s, 3H, OCH₃), 6.94 (d, 1H, Ar, J = 7.6 Hz), 7.30–7.35 (m, 2H, Ar), 7.38 (t, 1H, Ar, J = 7.2 Hz), 8.33 (d, 1H, Ar, J = 1.6 Hz), 8.47 (s, 1H, Ar), 8.69 (d, 1H, Ar, J = 1.6 Hz), 12.91 (exch br s, 1H, NH). IR ν (cm⁻¹): 2220 (CN). ESI-MS calcd. For C₁₅H₁₁N₃O, 249.27; found: m/z 250.09 [M+H]⁺. Anal. C₁₅H₁₁N₃O (C, H, N).

5-(6-Methoxynaphthalen-2-yl)-1H-pyrrolo[2,3-b]pyridine-3-carbonitrile (13e). Yield = 63%; mp = 193–196 °C (EtOH). $^1\text{H-NMR}$ (DMSO- d_6) δ 3.88 (s, 3H, OCH₃), 7.14–7.19 (m, 1H, Ar), 7.35 (s, 1H, Ar), 7.91–7.99 (m, 3H, Ar), 8.28 (s, 1H, Ar), 8.43–8.50 (m, 2H, Ar), 8.82 (s, 1H, Ar), 12.89 (exch br s, 1H, NH). IR ν (cm⁻¹): 2221 (CN). ESI-MS calcd. For C₁₉H₁₃N₃O, 299.33; found: m/z 300.11 [M+H]⁺. Anal. C₁₉H₁₃N₃O (C, H, N).

5-(Thiophen-3-yl)-1H-pyrrolo[2,3-b]pyridine-3-carbonitrile (13f). Yield = 88%; mp = 165–167 °C (EtOH). $^1\text{H-NMR}$ (DMSO- d_6) δ 7.67–7.73 (m, 2H, Ar), 8.05 (s, 1H, Ar), 8.39–8.44 (m, 2H, Ar), 8.80 (s, 1H, Ar), 12.86 (exch br s, 1H, NH). IR ν (cm⁻¹): 2222 (CN). ESI-MS calcd. For C₁₂H₇N₃S, 225.27; found: m/z 226.04 [M+H]⁺. Anal. C₁₂H₇N₃S (C, H, N).

5-(Pyridin-3-yl)-1H-pyrrolo[2,3-b]pyridine-3-carbonitrile (13g). Yield = 71%; mp = 285–287 °C dec (EtOH). (DMSO- d_6) δ 7.44–7.49 (m, 1H, Ar), 8.18 (d, 1H, Ar, J = 6.0 Hz), 8.40 (s, 1H, Ar), 8.47 (s, 1H, Ar), 8.57 (s, 1H, Ar), 8.73 (s, 1H, Ar), 8.97 (s, 1H, Ar), 12.96 (exch br s, 1H, NH). IR ν (cm⁻¹): 2220 (CN). ESI-MS calcd. For C₁₃H₈N₄, 220.23; found: m/z 221.08 [M+H]⁺. Anal. C₁₃H₈N₄ (C, H, N).

General procedure for compounds 14a–g. Compounds 14a–g were obtained following the same procedure reported for compounds 7a–c, but starting with intermediates 13a–g. The crude products were purified by column chromatography using cyclohexane/ethyl acetate 5:1 (for 14a–e), cyclohexane/ethyl acetate 4:1 (for 14f), or cyclohexane/ethyl acetate 1:3 (for 14g) as eluents.

1-(3-Methylbenzoyl)-5-phenyl-1H-pyrrolo[2,3-b]pyridine-3-carbonitrile (14a). Yield = 17%; mp = 160–163 °C (EtOH). $^1\text{H-NMR}$ (CDCl₃- d_1) δ 2.45 (s, 3H, m-CH₃-Ph), 7.40–7.45 (m, 2H, Ar), 7.51 (t, 3H, Ar, J = 7.2 Hz), 7.61 (t, 3H, Ar, J = 7.6 Hz), 7.68 (s, 1H, Ar), 8.24 (s, 1H, Ar), 8.26 (d, 1H, Ar, J = 2.0 Hz), 8.68 (d, 1H, Ar, J = 2.0 Hz). $^{13}\text{C-NMR}$ (CDCl₃- d_1) δ 20.93 (CH₃), 101.18 (C), 115.32 (C), 123.82 (CH), 127.54 (CH), 128.17 (CH), 130.86 (CH), 134.56 (CH), 136.41 (C), 138.83 (C), 144.65 (C), 167.76 (CO). IR ν (cm⁻¹): 2220 (CN). ESI-MS calcd. For C₂₂H₁₅N₃O, 337.37; found: m/z 338.12 [M+H]⁺. Anal. C₂₂H₁₅N₃O (C, H, N).

1-(3-Methylbenzoyl)-5-(3-[trifluoromethyl]phenyl)-1H-pyrrolo[2,3-b]pyridine-3-carbonitrile (14b). Yield = 10%; mp = 155–157 °C (EtOH). $^1\text{H-NMR}$ (CDCl₃- d_1) δ 2.46 (s, 3H, m-CH₃-Ph), 7.43 (t, 1H, Ar, J = 7.6 Hz), 7.52 (d, 1H, Ar, J = 8.0 Hz), 7.58–7.71 (m, 4H, Ar), 7.80 (d, 1H, Ar,

$J = 7.6$ Hz), 7.85 (s, 1H, Ar), 8.28 (s, 2H, Ar), 8.67 (d, 1H, Ar, $J = 2.0$ Hz). $^{13}\text{C-NMR}$ ($\text{CDCl}_3\text{-}d_1$) δ 21.31 (CH_3), 103.41 (C), 115.62 (C), 121.42 (CH), 124.75 (CH), 125.18 (CH), 126.74 (CH), 128.96 (CH), 129.56 (CH), 130.48 (CH), 130.92 (CH), 136.72 (C), 138.92 (C), 144.67 (C), 167.48 (CO). IR ν (cm^{-1}): 2220 (CN). ESI-MS calcd. For $\text{C}_{23}\text{H}_{14}\text{F}_3\text{N}_3\text{O}$, 405.37; found: m/z 406.11 $[\text{M}+\text{H}]^+$. Anal. $\text{C}_{23}\text{H}_{14}\text{F}_3\text{N}_3\text{O}$ (C, H, N).

1-(3-Methylbenzoyl)-5-(*m*-tolyl)-1H-pyrrolo[2,3-*b*]pyridine-3-carbonitrile (14c). Yield = 10%; mp = 115–118 °C (EtOH). $^1\text{H-NMR}$ ($\text{CDCl}_3\text{-}d_1$) δ 2.45 (s, 6H, 2 \times *m*- $\text{CH}_3\text{-Ph}$), 7.24 (s, 1H, Ar), 7.38–7.43 (m, 4H, Ar), 7.51 (d, 1H, Ar, $J = 7.2$ Hz), 7.59 (d, 1H, Ar, $J = 7.2$ Hz), 7.67 (s, 1H, Ar), 8.23 (s, 1H, Ar), 8.25 (d, 1H, Ar, $J = 2.0$ Hz), 8.67 (d, 1H, Ar, $J = 2.0$ Hz). $^{13}\text{C-NMR}$ ($\text{CDCl}_3\text{-}d_1$) δ 21.39 (CH_3), 21.56 (CH_3), 90.72 (C), 113.51 (C), 121.17 (C), 124.55 (CH), 126.66 (CH), 127.26 (CH), 127.83 (CH), 128.22 (CH), 128.45 (CH), 129.06 (CH), 129.18 (CH), 131.03 (CH), 132.07 (C), 134.31 (CH), 134.88 (CH), 137.30 (C), 138.75 (C), 139.03 (C), 146.04 (CH), 146.35 (C), 166.72 (CO). IR ν (cm^{-1}): 2220 (CN). ESI-MS calcd. For $\text{C}_{23}\text{H}_{17}\text{N}_3\text{O}$, 351.40; found: m/z 352.14 $[\text{M}+\text{H}]^+$. Anal. $\text{C}_{23}\text{H}_{17}\text{N}_3\text{O}$ (C, H, N).

5-(3-Methoxyphenyl)-1-(3-methylbenzoyl)-1H-pyrrolo[2,3-*b*]pyridine-3-carbonitrile (14d). Yield = 10%; mp = 152–155 °C (EtOH). $^1\text{H-NMR}$ ($\text{CDCl}_3\text{-}d_1$) δ 2.45 (s, 3H, *m*- $\text{CH}_3\text{-Ph}$), 3.88 (s, 3H, OCH_3), 6.97 (d, 1H, Ar, $J = 8.0$ Hz), 7.13–7.20 (m, 2H, Ar), 7.41 (d, 2H, Ar, $J = 7.6$ Hz), 7.51 (d, 1H, Ar, $J = 7.2$ Hz), 7.60 (d, 1H, Ar, $J = 7.2$ Hz), 7.67 (s, 1H, Ar), 8.25 (d, 2H, Ar, $J = 7.6$ Hz), 8.67 (s, 1H, Ar). $^{13}\text{C-NMR}$ ($\text{CDCl}_3\text{-}d_1$) δ 21.18 (CH_3), 55.76 (CH_3), 102.47 (C), 113.48 (CH), 114.39 (CH), 115.49 (C), 119.82 (CH), 121.43 (C), 123.64 (CH), 126.12 (CH), 128.17 (CH), 129.32 (CH), 130.14 (CH), 131.18 (C), 134.56 (CH), 138.97 (C), 144.65 (C), 161.18 (C), 168.71 (CO). IR ν (cm^{-1}): 2220 (CN). ESI-MS calcd. For $\text{C}_{23}\text{H}_{17}\text{N}_3\text{O}_2$, 367.40; found: m/z 368.14 $[\text{M}+\text{H}]^+$. Anal. $\text{C}_{23}\text{H}_{17}\text{N}_3\text{O}_2$ (C, H, N).

5-(6-Methoxynaphthalen-2-yl)-1-(3-methylbenzoyl)-1H-pyrrolo[2,3-*b*]pyridine-3-carbonitrile (14e). Yield = 22%; oil. $^1\text{H-NMR}$ ($\text{CDCl}_3\text{-}d_1$) δ 2.46 (s, 3H, *m*- $\text{CH}_3\text{-Ph}$), 3.95 (s, 3H, OCH_3), 7.18–7.25 (m, 2H, Ar), 7.43 (t, 1H, Ar, $J = 7.6$ Hz), 7.51 (d, 1H, Ar, $J = 7.2$ Hz), 7.61 (d, 1H, Ar, $J = 7.2$ Hz), 7.68–7.73 (m, 2H, Ar), 7.81–7.88 (m, 2H, Ar), 8.00 (s, 1H, Ar), 8.25 (s, 1H, Ar), 8.36 (s, 1H, Ar), 8.79 (s, 1H, Ar). $^{13}\text{C-NMR}$ ($\text{CDCl}_3\text{-}d_1$) δ 21.19 (CH_3), 55.85 (CH_3), 101.06 (C), 105.92 (CH), 113.49 (CH), 114.39 (C), 115.41 (C), 119.87 (CH), 121.43 (C), 123.68 (CH), 125.44 (CH), 126.15 (CH), 128.17 (CH), 129.35 (CH), 129.60 (CH), 130.14 (CH), 131.11 (C), 134.56 (CH), 134.82 (C), 138.91 (C), 144.62 (C), 157.28 (C), 167.70 (CO). IR ν (cm^{-1}): 2220 (CN). ESI-MS calcd. For $\text{C}_{27}\text{H}_{19}\text{N}_3\text{O}_2$, 417.46; found: m/z 418.15 $[\text{M}+\text{H}]^+$. Anal. $\text{C}_{27}\text{H}_{19}\text{N}_3\text{O}_2$ (C, H, N).

1-(3-Methylbenzoyl)-5-(thiophen-3-yl)-1H-pyrrolo[2,3-*b*]pyridine-3-carbonitrile (14f). Yield = 40%; mp = 171–173 °C (EtOH). $^1\text{H-NMR}$ ($\text{CDCl}_3\text{-}d_1$) δ 2.45 (s, 3H, *m*- $\text{CH}_3\text{-Ph}$), 7.42 (d, 2H, Ar, $J = 7.2$ Hz), 7.47–7.52 (m, 2H, Ar), 7.54–7.59 (m, 2H, Ar), 7.66 (s, 1H, Ar), 8.22 (s, 1H, Ar), 8.25 (d, 1H, Ar, $J = 2.0$ Hz), 8.71 (d, 1H, Ar, $J = 2.0$ Hz). $^{13}\text{C-NMR}$ ($\text{CDCl}_3\text{-}d_1$) δ 21.35 (CH_3), 90.66 (C), 113.42 (C), 121.22 (C), 121.75 (CH), 125.68 (CH), 126.07 (CH), 127.36 (CH), 127.80 (CH), 128.41 (CH), 129.05 (C), 130.99 (CH), 132.08 (C), 132.08 (CH), 135.33 (CH), 138.25 (C), 138.72 (C), 145.36 (CH), 146.09 (C), 166.64 (CO). IR

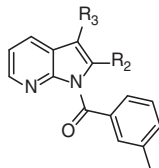
ν (cm^{-1}): 2222 (CN). ESI-MS calcd. For $\text{C}_{20}\text{H}_{13}\text{N}_3\text{OS}$, 343.40; found: m/z 344.08 $[\text{M}+\text{H}]^+$. Anal. $\text{C}_{20}\text{H}_{13}\text{N}_3\text{OS}$ (C, H, N).

1-(3-Methylbenzoyl)-5-(pyridin-3-yl)-1H-pyrrolo[2,3-*b*]pyridine-3-carbonitrile (14g). Yield = 32%; mp = 155–157 °C (EtOH). $^1\text{H-NMR}$ ($\text{CDCl}_3\text{-}d_1$) δ 2.44 (s, 3H, *m*- $\text{CH}_3\text{-Ph}$), 7.40–7.67 (m, 5H, Ar), 7.93 (d, 1H, Ar, $J = 6.0$ Hz), 8.27 (s, 2H, Ar), 8.67 (d, 2H, Ar, $J = 7.6$ Hz), 8.88 (s, 1H, Ar). $^{13}\text{C-NMR}$ ($\text{CDCl}_3\text{-}d_1$) δ 21.32 (CH_3), 90.71 (C), 113.22 (C), 121.28 (C), 123.57 (CH), 126.84 (CH), 126.98 (CH), 127.85 (CH), 128.47 (CH), 130.83 (C), 131.02 (CH), 131.92 (C), 133.19 (C), 134.83 (CH), 135.02 (CH), 138.81 (C), 145.54 (CH), 145.77 (CH), 146.76 (C), 149.27 (CH), 166.56 (CO). IR ν (cm^{-1}): 2220 (CN). ESI-MS calcd. For $\text{C}_{21}\text{H}_{14}\text{N}_4\text{O}$, 338.36; found: m/z 339.12 $[\text{M}+\text{H}]^+$. Anal. $\text{C}_{21}\text{H}_{14}\text{N}_4\text{O}$ (C, H, N).

2.3 | Pharmacology

Compounds were dissolved in 100% DMSO at 5 mM stock concentrations. The final concentration of DMSO in the reactions was 1%, and this level of DMSO had no effect on HNE activity. The HNE inhibition assay was performed in black flat-bottom 96-well microtiter plates. Briefly, a buffer solution containing 200 mM Tris-HCl, pH 7.5, 0.01% bovine serum albumin, 0.05% Tween-20, and 20 mU/mL HNE (Calbiochem) was added to wells containing different concentrations of each compound. The reactions were initiated by addition of 25 μM elastase substrate (N-methylsuccinyl-Ala-Ala-Pro-Val-7-amino-4-methylcoumarin, Calbiochem) in a final reaction volume of 100 μL /well. Kinetic measurements were obtained every 30 s for 10 min at 25 °C using a Fluoroskan Ascent FL fluorescence microplate reader (Thermo Electron, MA) with excitation and emission wavelengths at 355 and 460 nm, respectively. For all compounds tested, the concentration of inhibitor that caused 50% inhibition of the enzymatic reaction (IC_{50}) was calculated by

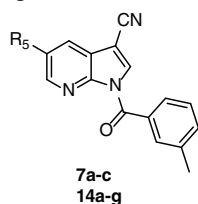
TABLE 1 HNE inhibitory activity of 1H-pyrrolo[2,3-*b*]pyridine derivatives 2a-e

| Compound |  | | IC_{50} (μM) ^a |
|----------------|---|----------------|---|
| | R ₂ | R ₃ | |
| 2a | CH_3 | H | N.A. ^b |
| 2b | CH_2CH_3 | H | N.A. ^b |
| 2c | COOEt | H | N.A. ^b |
| 2d | CN | H | 3.5 ± 1.2 |
| 2e | CH_3 | CN | 10.8 ± 2.2 |
| X ^c | H | CN | 0.015 ± 0.004 |
| Sivelestat | | | 0.050 ± 0.020 |

^a IC_{50} values are presented as the mean \pm SD of three independent experiment with a 6-point dilution series for each experiment.

^bNA: no inhibitory activity was found at the highest concentration of compound tested (50 μM).

^cCrocetti et al., 2018.

TABLE 2 HNE inhibitory activity of 1H-pyrrolo[2,3-b]pyridine derivatives **7a-c** and **14a-g**

| Compound | R ₅ | IC ₅₀ (μM) ^a |
|----------------|---------------------------------|------------------------------------|
| 7a | Br | 0.051 ± 0.014 |
| 7b | Cl | 0.16 ± 0.05 |
| 7c | NO ₂ | 0.40 ± 0.11 |
| 14a | Ph | 0.050 ± 0.02 |
| 14b | m-CF ₃ Ph | 0.18 ± 0.07 |
| 14c | m-CH ₃ Ph | 0.13 ± 0.04 |
| 14d | m-OCH ₃ Ph | 0.070 ± 0.015 |
| 14e | 6-OCH ₃ -naphthalene | 1.6 ± 0.33 |
| 14f | 3-thienyl | 0.042 ± 0.015 |
| 14g | 3-pyridyl | 0.015 ± 0.004 |
| X ^b | H | 0.015 ± 0.004 |
| Sivelestat | – | 0.050 ± 0.020 |

^aIC₅₀ values are presented as the mean ± SD of three independent experiments with a 6-point dilution series for each experiment.

^bCrocetti et al., 2018.

plotting % inhibition versus logarithm of inhibitor concentration (at least six points). The data are presented as the mean values of at least three independent experiments with relative standard deviations of <15%.

2.4 | Molecular modeling

Initial 3D structures of the compounds were generated with ChemOffice Professional (Perkin Elmer, Waltham, MA) and refined by the semiempirical PM3 method using HyperChem 8.0 (Shimadzu Corporation, Kyoto, Japan). Docking computations were performed using Molegro Virtual Docker (MVD), version 6.0 (CLC Bio, Copenhagen, Denmark), as described previously (Crocetti et al., 2013). The

structure of HNE co-crystallized with a peptide chloromethyl ketone inhibitor (1HNE entry of the Protein Data Bank) (Navia et al., 1989) was used for the docking study. The search area was chosen as a sphere of 10 Å radius centered at the nitrogen atom in the five-membered ring of the co-crystallized inhibitor. This peptide and co-crystallized water molecules were removed from the 1HNE structure, and side chain flexibility was set for the 42 residues closest to the center of the sphere (Crocetti et al., 2013), including the following residues surrounding the HNE binding site (i.e., located in the vicinity of the co-crystallized inhibitor): His57, Cys58, Leu99B, Val190, Cys191, Phe192, Gly193, Asp194, Ser195, Ala213, Ser214, Phe215, and Val216. For each compound, 15 docking runs were performed with full flexibility of the ligand around all rotatable bonds and side chain flexibility of the above-mentioned residues of the enzyme. Docking poses with the lowest docking score of each compound were checked for the ability to form a Michaelis complex between the Ser195 hydroxyl group and the carbonyl moiety in a ligand. In brief, the d_1 values [distance O(Ser195)···C between the Ser195 hydroxyl oxygen atom and the ligand carbonyl carbon atom closest to O(Ser195)] and α [angle O(Ser195)···CO, where CO is the carbonyl group of a ligand closest to O(Ser195)] were measured for each docked compound (Peters & Merz, 2006). The ability of proton transfer from Ser195 to Asp102 via His57 (the key catalytic triad of serine proteases) was also estimated by determining distances d_2 between the NH nitrogen in His57 and carboxyl oxygen atoms in Asp102, as described previously (Crocetti et al., 2013). The distance between the pyridine-type nitrogen in His57 and the OH proton in Ser195 is also important for proton transfer. However, because of easy rotation of the Ser195 OH group about the C—O bond, we measured distance d_3 between the Ser195 oxygen atom and the basic nitrogen atom in His57. The effective length L of the proton transfer channel was determined as $L = d_3 + \min(d_2)$.

3 | RESULTS AND DISCUSSION

All new products were tested for their ability to inhibit HNE, and the experiments were conducted in triplicate using *N*-methylsuccinyl-Ala-Ala-Pro-Val-7-amino-4-cumarin as the substrate. The results are reported in the Tables 1 and 2 and are compared with the Sivelestat

TABLE 3 Geometric parameters of the enzyme-inhibitor complexes predicted by molecular docking^a

| Compound | IC ₅₀ (μM) | d_1 (Å) | α (degree) | d_3 (Å) | d_2 (Å) | L (Å) ^b |
|----------------|-----------------------|-----------|-------------------|-----------|--------------|----------------------|
| X ^c | 0.015 | 2.601 | 117.0 | 3.302 | 3.218, 4.390 | 6.520 |
| 2d | 3.5 | 3.562 | 41.1 | 2.600 | 2.477, 3.562 | 5.077 |
| 2e | 10.8 | 3.342 | 117.23 | 3.535 | 5.355, 6.141 | 8.890 |
| 14c | 0.05 | 3.084 | 67.33 | 2.466 | 3.964, 5.421 | 6.430 |
| 14g | 0.015 | 4.364 | 117.9 | 3.007 | 4.143, 2.945 | 5.952 |

^aThe geometric parameters important for formation of a Michaelis complex in the HNE active site are as reported previously (Crocetti et al., 2011), based on the model of synchronous proton transfer from the oxyanion hole in HNE (Groutas et al., 1997). According to the docking results, a Michaelis complex with Ser195 is formed with participation of the ester carbonyl group.

^bLength of the channel for proton transfer calculated as $d_3 + \min(d_2)$.

^cCrocetti et al., 2018.

and 1-(3-methylbenzoyl)-1H-pyrrolo[2,3-b]pyridine-3-carbonitrile (compound **X**), which we previously found to be a potent HNE inhibitor (Crocetti et al., 2018). As shown in Table 1, the introduction of substituents at position 2 of the pyrrolo[2,3-b]pyridine scaffold was not favorable for HNE inhibitory activity. In fact, introduction of an alkyl group (compounds **2a** and **2b**) or a carbethoxy group (**2c**) led to products completely devoid of activity. In addition, shift of the carbonitrile group from position 3 of compound **X** to position 2 (**2d**) also led to a significant loss in HNE inhibitory activity (two orders of magnitude lower). Likewise, the introduction of a methyl group at position 2 of compound **X** was detrimental for activity, resulting in **2e** with an IC_{50} of 10.8 μ M, further confirming that substituents at position 2 are not tolerated without significant loss in HNE inhibitory activity.

In contrast, position 5 was more tolerant to substitutions, as most of the 5-substituted pyrrolo[2,3-b]pyridines exhibited IC_{50} values in the nanomolar range (0.015–0.070 μ M) (see Table 2). The 5-bromine derivative was about threefold more potent (**7a**, IC_{50} = 0.051 μ M) than the 5-chloro (**7b**, IC_{50} = 0.160 μ M) derivative, suggesting that lipophilicity (π = 0.86 for Br and 0.71 for Cl), steric bulk (Mr = 8.88 for Br and 6.03 for Cl), or electron withdrawing ability could be important requirements for activity. On the other hand, the introduction of a nitro group (**7c**), which has an intermediate Mr between bromine and chlorine (Mr = 7.36) but hydrophilic properties (π = −0.28) was about twofold less potent than the 5-chloro derivative **7b** (IC_{50} = 0.400 and 0.160 μ M, respectively).

Insertion of bulky and lipophilic rings was favorable for HNE inhibitory activity within certain limits, as demonstrated by the comparable potency of the 5-(substituted)phenyl derivatives **14a–d** (IC_{50} = 0.050–0.180 μ M) and the low activity of compound **14e** bearing a 6-OCH₃-naphthalen at position 5 (IC_{50} = 1.6 μ M). Replacement of the phenyl at position 5 in compound **14a** with the isostere thienyl or pyridyl rings resulted in the thienyl derivative **14f** with comparable potency to **14a** (IC_{50} = 0.042 versus 0.050 μ M, respectively) and the pyridyl derivative **14g**, which was about threefold more potent than **14a** (IC_{50} = 0.015 versus 0.050 μ M, respectively). Thus, the presence of pyridine in compound **14g** may be important not only for steric hindrance but also for the formation of an H-bond that involves a nitrogen atom, which is not found in **14a**.

Taking into account these biological results and in particular the observation that the most potent 5-substituted compound (**14g**) exhibited the same IC_{50} as the 5-unsubstituted lead compound **X**, we can conclude that the introduction of certain substituents at position 5 maintained HNE inhibitory activity, probably by interacting with the large pocket of the enzyme site. On the other hand, we were not able to improve the HNE inhibitory activity with respect the lead **X**.

The difference in activities of the test compounds can be explained by the length L of the proton transfer channel, angle α , and length d_1 . As reported previously, a nitrogen atom in the six-membered pyridine moiety of the lead **X** forms an H-bond with Asp194 (Crocetti et al., 2018). Additional H-bonding occurs with Val216 due to the nitrogen atom of the cyano group in lead compound **X** (Crocetti et al., 2018). The distance d_1 for molecule **X** is smaller than for other active compounds in Table 3. In general, the

geometry of the inhibitor-enzyme complex is favorable for the formation of a Michaelis complex when the oxygen atom of Ser195 attacks the carbonyl carbon atom of compound **X**.

Although compound **2e** has distance d_1 and angle α suitable for inhibitory activity, arrangement of the amino acid residues of the key triad Ser195-His57-Asp102 becomes unfavorable because the length L of the proton transfer channel is greatly increased (Table 3), which may be the main reason for the low inhibitory activity of compound **2e**, despite the formation of H-bonds with Ser195 and Gly193

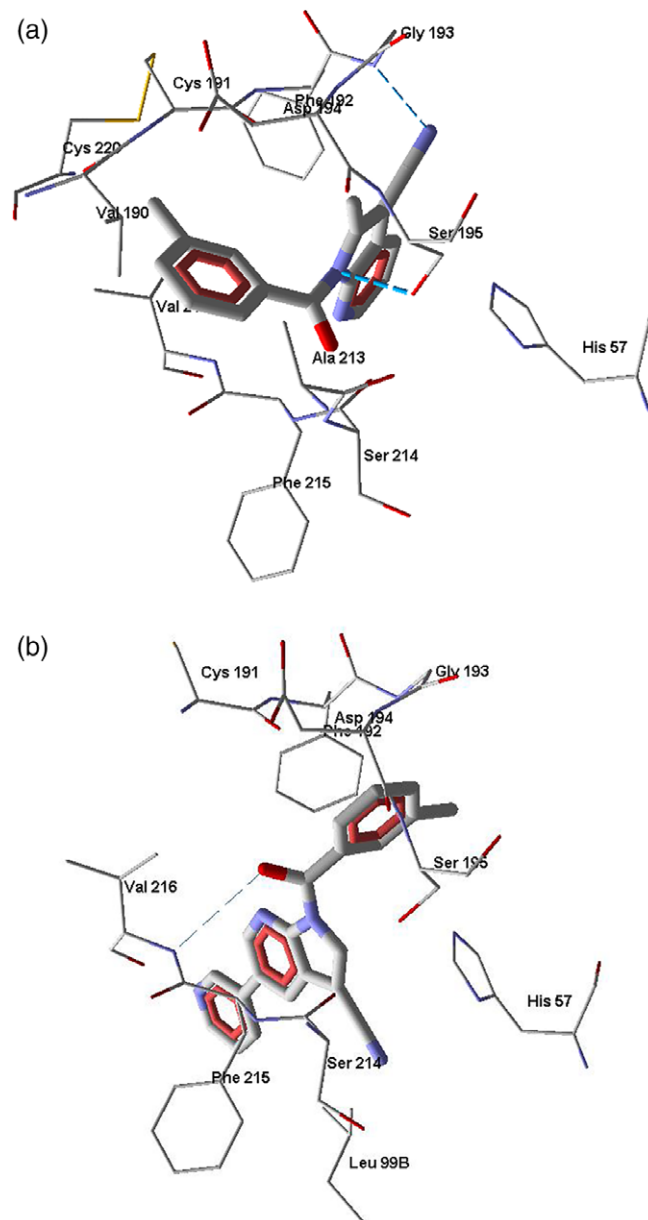


FIGURE 5 Docking poses of inhibitors **2e** and **14g** based on the pyrrolo[2,3-b]pyridine scaffold in the human neutrophil elastase binding site (1HNE entry of Protein Data Bank). Panel (a) Docking pose of molecule **2e**. Ser195 is H-bonded to amide nitrogen atom, while the cyano group forms a hydrogen bond with Gly193. Panel (b) Docking pose of molecule **14g**. The carbonyl oxygen atom forms a hydrogen bond with Val216. Residues within 4 Å from each pose are shown

involving two nitrogen atoms (Figure 5a). Although compound **2d** has a short length *L*, it has strong anchoring due to H-bonding of the carbonyl oxygen with Ser195 of the catalytic triad (not shown). Clearly, significant fixation of the molecule at the binding site leads to unfavorable activity (i.e., angle α is too acute for compound **2d**, see Table 3). This may cause difficulties in formation of the Michaelis complex and, therefore, reduced activity of **2d**. It should be noted that the cyano group at position 2 does not form H-bonds with the enzyme, in contrast with the same group at position 3 of molecule **X**.

As for the highly active HNE inhibitors **14c** and **14g**, the geometric parameters of the docking poses, as well as the distance *L*, were favorable for the formation of Michaelis complexes and for proton transfer via the catalytic triad (Table 3). It should be noted that the angle α for compound **14c** falls slightly out of the optimal interval 80–120° (Groutas et al., 1997; Vergely et al., 1996), which can explain the reduced inhibitory activity in comparison with inhibitor **14g**. Molecules **14c** and **14g** are fixed within the HNE binding site by H-bonds in the above-mentioned orientations that are favorable for biological activity (Figure 5b). Thus, the geometrical parameters of the docking poses found with flexible side chains of the enzyme allow us to explain the differences in inhibitory activity of the investigated compounds.

4 | CONCLUSIONS

In the present study, we further investigated the pyrrolo[2,3-*b*]pyridine scaffold, which was previously found to be suitable for the synthesis of HNE inhibitors (IC_{50} = 14–87 nM) (Crocetti et al., 2018). While maintaining the best substituents identified for N-1 and position 3 (m-toluoyl and CN groups, respectively), we introduced substituents with different features at position 5 in order to assess the impact of these modifications on binding and HNE inhibition. Moreover, we also evaluated modification of the substituent at position 2 of the scaffold. The biological results clearly demonstrated that position 2 of the pyrrolo[2,3-*b*]pyridine scaffold must be unsubstituted, whereas the introduction of certain substituents at position 5 maintained HNE inhibitory activity comparable with that of reference compound **X**, probably by interacting with the large pocket of the enzyme site. According to our molecular modeling, the most active HNE inhibitors bind the enzyme in conformations suitable for the formation of a Michaelis complex between the ligand C=O group and Ser195. Additionally, for the potent inhibitors, a mutual orientation of the ligand with the catalytic triad is necessary for effective proton transfer from the oxyanion hole.

ACKNOWLEDGMENTS

This research was supported in part by National Institutes of Health IDeA Program COBRE Grant GM110732; USDA National Institute of Food and Agriculture Hatch project 1009546; Montana University System Research Initiative: 51040-MUSRI2015-03; Tomsk Polytechnic University Competitiveness Enhancement Program; Ministry of Education

and Science of the Russian Federation project No. 4.8192.2017/8.9, and the Montana State University Agricultural Experiment Station.

ORCID

Letizia Crocetti  <https://orcid.org/0000-0003-3473-2683>

REFERENCES

- Bahekar, R. H., Jain, M. R., Jadavav, P. A., Projapati, V. M., Patel, D. N., Gupta, A. A., ... Modi, H. (2007). Synthesis and antidiabetic activity of 2,5-disubstituted-3-imidazol-2-yl-pyrrolo[2,3-*b*]pyridines. *Bioorganic & Medicinal Chemistry*, 15(21), 6782–6795.
- Baltus, C. B., Jorda, R., Marat, C., Berka, C., Bazgier, V., Krystal, V., ... Viad-Massuard, M. C. (2016). Synthesis, biological evaluation and molecular modeling of a novel series of 7-azaindole based tri-heterocyclic compounds as potent CDK2/cyclin E inhibitors. *European Journal of Medicinal Chemistry*, 108, 701–719.
- Bhat, P. V., Dere, R. T., Ravikumar, S., Hindupur, R. M., & Pati, H. N. (2015). Efficient and scalable process for synthesis of 5-nitro-7-azaindole. *Organic Process Research and Development*, 19, 1282–1285.
- Chen, G., Ren, H., Zhang, N., Lennox, W., Turpoff, A., Paget, S., ... Gu, Z. (2015). (Azaindol-2-yl)pyridine-3-sulfonamides as potent and selective inhibitors targeting hepatitis C virus NS4B. *Bioorganic & Medicinal Chemistry Letters*, 25, 781–786.
- Crocetti, L., Giovannoni, M. P., Schepetkin, I. A., Quinn, M. T., Khlebnikov, A. I., Cantini, N., ... Vergelli, C. (2018). 1H-pyrrolo[2,3-*b*]pyridine: A new scaffold for human neutrophil elastase (HNE) inhibitor. *Bioorganic & Medicinal Chemistry*, 26, 5583–5595.
- Crocetti, L., Giovannoni, M. P., Schepetkin, I. A., Quinn, M. T., Khlebnikov, A. I., Cilibrizzi, A., ... Vergelli, C. (2011). Design, synthesis and evaluation of N-benzoylindazole derivatives and analogues as inhibitors of human neutrophil elastase. *Bioorganic & Medicinal Chemistry*, 19, 4460–4472.
- Crocetti, L., Schepetkin, I. A., Ciciani, G., Giovannoni, M. P., Guerrini, G., Iacovone, A., ... Vergelli, C. (2016). Synthesis and pharmacological evaluation of indole derivatives as deaza analogues of potent human neutrophil elastase inhibitors. *Drug Development Research*, 77(6), 285–289.
- Crocetti, L., Schepetkin, I. A., Cilibrizzi, A., Graziano, A., Vergelli, C., Giomi, D., ... Giovannoni, M. P. (2013). Optimization of N-benzoylindazole derivatives as inhibitors of human neutrophil elastase. *Journal of Medicinal Chemistry*, 56, 6259–6272.
- Ermoli, A., Bargiotti, A., Brasca, M. G., Ciavolella, A., Colombo, N., Fachin, G., ... Vanotti, E. (2009). Cell division cycle 7 kinase inhibitors: 1H-pyrrolo[2,3-*b*]pyridines, synthesis and structure–activity relationships. *Medicinal Chemistry*, 52, 4380–4390.
- Fujinaga, M., Chernaia, M. M., Halenbeck, R., Kothe, K., & James, M. N. G. (1996). The crystal structure of PR3, a neutrophil serine proteinase antigen of Wegener's granulomatosis antibodies. *Journal of Molecular Biology*, 261, 267–278.
- Giovannoni, M. P., Schepetkin, I. A., Crocetti, L., Ciciani, G., Cilibrizzi, A., Guerrini, G., ... Vergelli, C. (2016). Cinnoline derivatives as human neutrophil elastase inhibitors. *Journal of Enzyme Inhibition and Medicinal Chemistry*, 31(4), 628–639.
- Giovannoni, M. P., Schepetkin, I. A., Quinn, M. T., Cantini, N., Crocetti, L., Guerrini, G., ... Vergelli, C. (2018). Synthesis, biological evaluation, and molecular modelling studies of potent human neutrophil elastase (HNE) inhibitors. *Journal of Enzyme Inhibition and Medicinal Chemistry*, 33(1), 1108–1124.
- Graczyk, P., Palmer, V., & Khan, A. (2004). Preparation of 3-ethynyl or 3-cyano-1H-pyrrolo[2,3-*b*]pyridine derivatives as c-Jun N-terminal kinase (JNK) inhibitors. From PCT Int Appl WO 2004101565.

- Groutas, W. C., Kuang, R., Venkataraman, R., Epp, J. B., Ruan, S., & Prakash, O. (1997). Structure-based design of a general class of mechanism-based inhibitors of the serine proteinases employing a novel amino acid-derived heterocyclic scaffold. *Biochemistry*, 36, 4739–4750.
- Ibrahim, P. N., Artis, D. R., Bremer, R., Habets, G., Mamo, S., Nespi, M., ... West, B. (2007). Pyrrolo[2,3-b]pyridine derivatives as protein kinase inhibitors and their preparation, pharmaceutical compositions and use in the treatment of diseases. From PCT Int Appl WO 2007002433.
- Joydev, K. L., Rohan, A. B., & Mandeep Kaur, H. (2017). Intramolecular oxidative arylations in 7-azaindoles and pyrroles: Revamping the synthesis of fused N-heterocycle tethered fluorenes. *Chemistry: A European Journal*, 23, 2044–2050.
- Korkmaz, B., Horwitz, M. S., Jenne, D. E., & Gauthier, F. (2010). Neutrophil elastase, proteinase 3, and cathepsin G as therapeutic targets in human diseases. *Pharmacological Reviews*, 62, 726–759.
- Laha, J. K., Bhimpuria, R. A., & Hunjan, M. K. (2017). Intramolecular oxidative arylations in 7-azaindoles and pyrroles: Revamping the synthesis of fused n-heterocycle tethered fluorenes. *Chemistry: A European Journal*, 23, 2044–2050. <https://doi.org/10.1002/chem.201604192>
- Liu, N., Wang, Y., Huang, G., Ji, C., Fan, W., Li, H., ... Tian, H. (2016). Design, synthesis and biological evaluation of 1H-pyrrolo[2,3-b]pyridine and 1H-pyrazolo[3,4-b]pyridine derivatives as c-Met inhibitors. *Bioorganic Chemistry*, 65, 146–158.
- Lucas, S. D., Costa, E., Guedes, R. C., & Moreira, R. (2011). Targeting COPD: Advances on low-molecular-weight inhibitors of human neutrophil elastase. *Medicinal Research Reviews*, 33, E73–E101.
- Navia, M. A., McKeever, B. M., Springer, J. P., Lin, T. Y., Williams, H. R., Fluder, E. M., ... Hoogsteen, K. (1989). Structure of human neutrophil elastase in complex with a peptide chloromethyl ketone inhibitor at 1.84 Å resolution. *Proceedings of the National Academy of Sciences of the United States of America*, 86, 7–11.
- Nirogi, R., Shinde, A., Daulatabad, A., Kambhampati, R., Gudla, P., Shaik, M., ... Reballi, V. (2012). Design, synthesis, and pharmacological evaluation of piperidin-4-yl amino aryl sulfonamides: novel, potent, selective, orally active, and brain penetrant 5-HT₆ receptor antagonists. *Journal of Medicinal Chemistry*, 55, 9255–9269.
- Peters, M. B., & Merz, K. M. (2006). Semiempirical comparative binding energy analysis (SECOMBINE) of a series of trypsin inhibitors. *Journal of Chemical Theory and Computation*, 2, 383–399.
- Pham, C. T. (2006). Neutrophil serine proteases: Specific regulators of inflammation. *Nature Reviews. Immunology*, 6, 541–550.
- Pires, M. J. D., Poira, D. L., Purificacao, S. I., & Marques, M. M. B. (2016). Synthesis of substituted 4-, 5-, 6- and 7-azaindoles from aminopyridines via a cascade C-N cross-coupling/heck reaction. *Organic Letters*, 18(13), 3250–3253.
- Polverino, E., Rosales-Mayor, E., Dale, G. E., Dembowski, K., & Torres, A. (2017). The role of neutrophil Elastase inhibitors in lung diseases. *Chest*, 152(2), 249–262.
- Sandham, D. A., Adcock, C., Bala, K., Barker, L., Brown, Z., Dubois, G., ... Wilson, C. (2009). 7-Azaindole-3-acetic acid derivatives: Potent and selective CRTh2 receptor antagonists. *Bioorganic & Medicinal Chemistry*, 19, 4794–4798.
- Schepetkin, I. A., Khlebnikov, A. I., & Quinn, M. T. (2007). N-benzoylpyrazoles are novel small-molecule inhibitors of human neutrophil elastase. *Journal of Medicinal Chemistry*, 50, 4928–4938.
- Singh, U., Chashoo, G., Khan, S. U., Mahajan, P., Singh, A., Sharma, A., ... Singh, P. P. (2017). Design o novel 3-pyrimidinylazaindole CDK2/9 inhibitors with potent in vivo antitumor efficacy in a triple negative breast cancer model. *Journal of Medicinal Chemistry*, 60(23), 9470–9489.
- Vergelli, C., Schepetkin, I. A., Crocetti, L., Iacovone, A., Giovannoni, M. P., Guerrini, G., ... Quinn, M. T. (2017). Isoxazol-5(2H)-one: A new scaffold for potent human neutrophil elastase (HNE) inhibitors. *Journal of Enzyme Inhibition and Medicinal Chemistry*, 32(1), 821–831.
- Vergely, I., Laugaa, P., & Reboud-Ravaux, M. (1996). Interaction of human leukocyte elastase with a N-aryl azetidinone suicide substrate: Conformational analyses based on the mechanism of action of serine proteinases. *Journal of Molecular Graphics*, 14(3), 158–167.
- Von Nussbaum, F., & Li, V. M. J. (2015). Neutrophil elastase inhibitors for the treatment of (cardio)pulmonary diseases: Into clinical testing with pre-adaptive pharmacophores. *Bioorganic & Medicinal Chemistry Letters*, 25, 4370–4381.
- Von Nussbaum, F., Li, V. M. J., Daniel Meibom, D., Anlauf, S., Bechem, M., Delbeck, M., ... Schamberger, J. (2016). Potent and selective human neutrophil elastase inhibitors with novel equatorial ring topology: in vivo efficacy of the polar pyrimidopyridazine BAY-8040 in a pulmonary arterial hypertension rat model. *ChemMedChem*, 11, 199–206.
- Xi, N., & Li, X. (2014). Preparation of alkenyl-pyrrolo[2,3-b]pyridine compounds as protein tyrosine kinase modulators useful for treatment of proliferative disorders. From PCT Int Appl WO 2014193647.
- Zhong, Q. Q., Wang, X., Li, Y. F., Peng, L. J., & Jiang, Z. S. (2017). Secretory leukocyte protease inhibitor promising protective roles in obesity-associated atherosclerosis. *Experimental Biology and Medicine*, 242(3), 250–257.

How to cite this article: Giovannoni MP, Cantini N, Crocetti L, et al. Further modifications of 1H-pyrrolo[2,3-b]pyridine derivatives as inhibitors of human neutrophil elastase. *Drug Dev Res*. 2019;1–12. <https://doi.org/10.1002/ddr.21539>